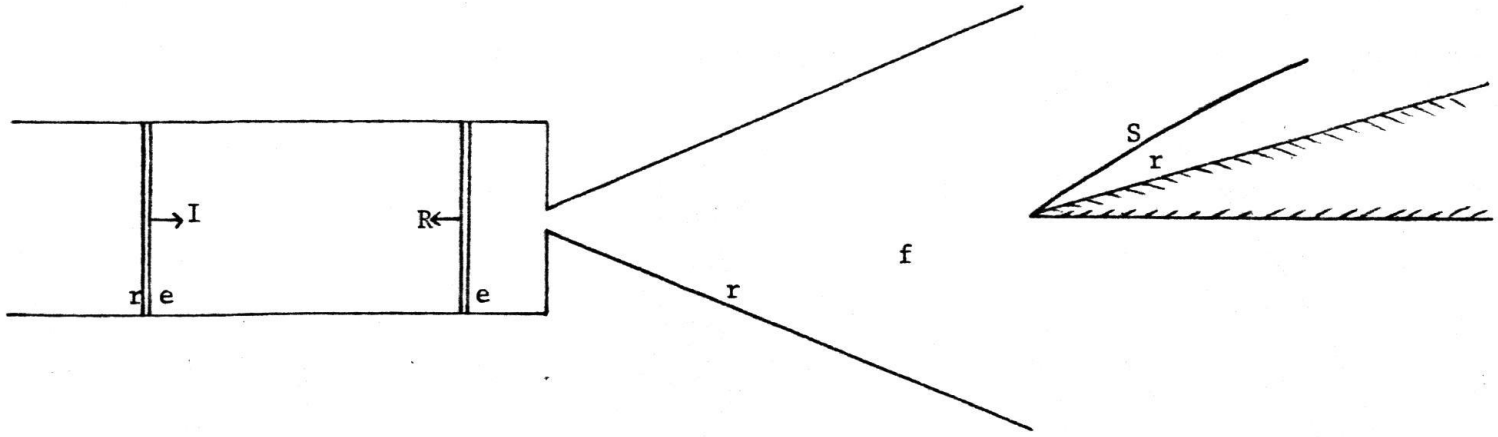

Figure 1.1: A schematic diagram of a shock tunnel

I represents the initial shock into an equilibrium test gas.

R represents the reflected shock with an equilibrium nozzle reservoir behind it.

S represents the standing shock on a wedge in a nonequilibrium test gas.

e denotes equilibrium conditions

f denotes frozen conditions

r denotes relaxing conditions

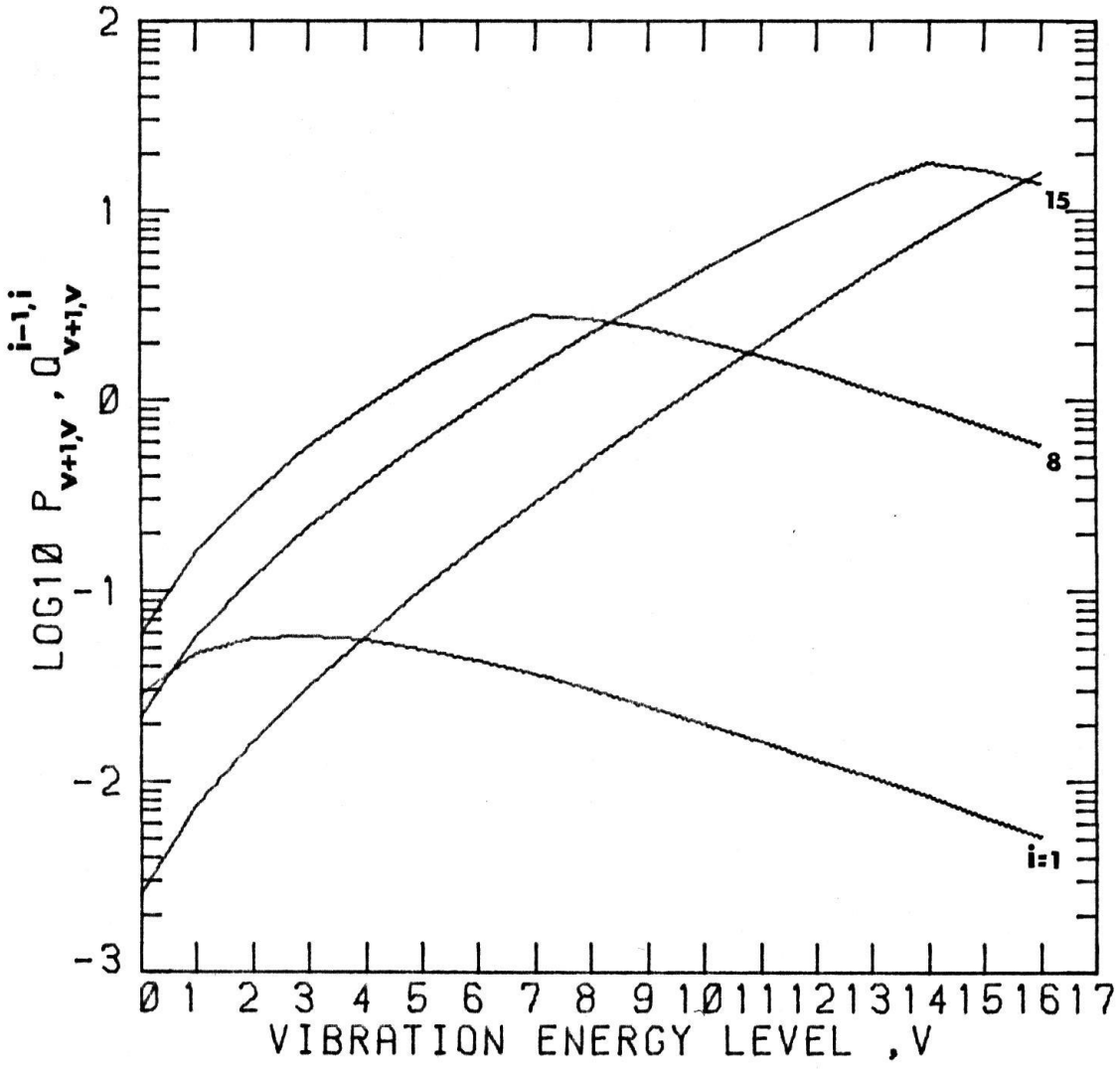

Figure 2.1: Vibrational transition probabilities for H_2 at 5000K and 1 atm.

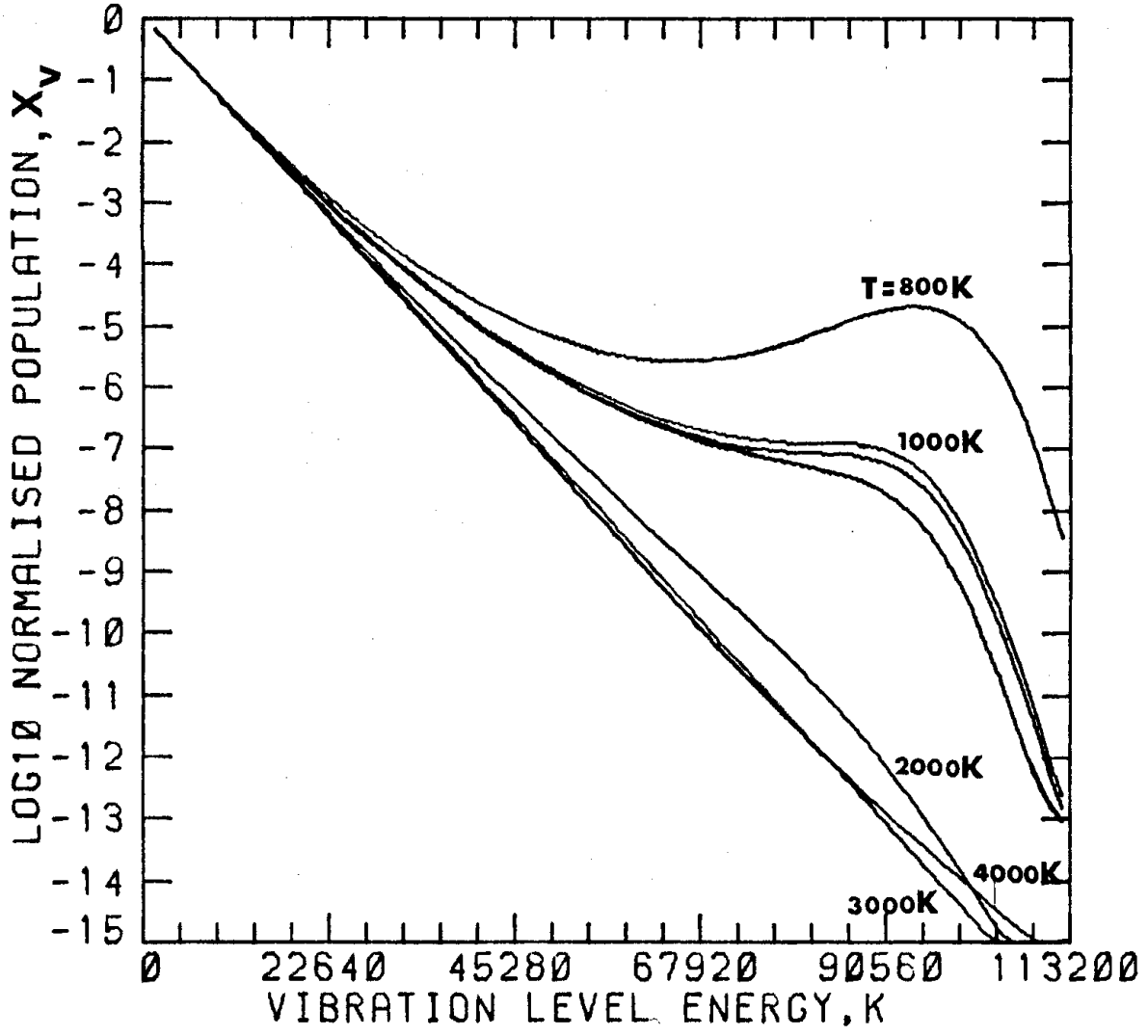

Figure 2.2: Vibrational level population distribution for N_2 at 1 atm and Y = 3000K. The translational temperature varies from 4000 to 800K. The two curves just below T = 1000K correspond to values of -3×10^{5} and $-3\times10^{6}Ks^{-1}$ for $\frac{dT}{dt}$, respectively.

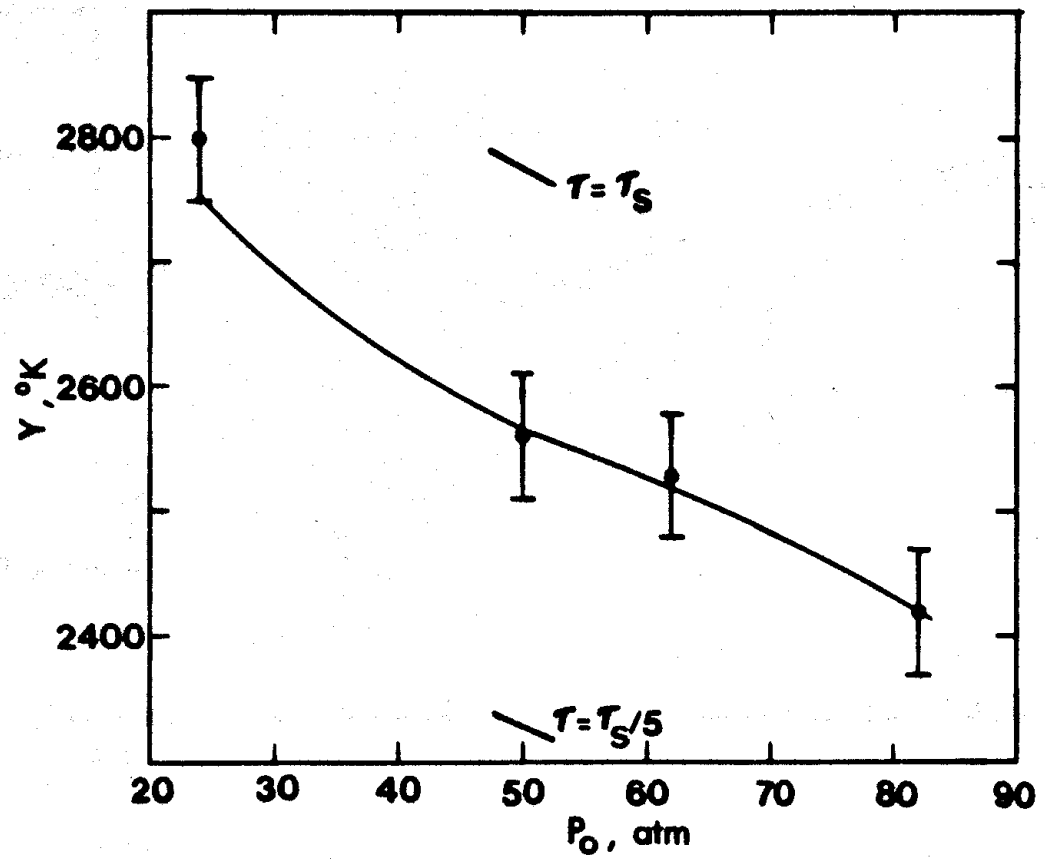

Figure 2.3: Vibrational temperature (Y) vs reservoir pressure (P_o) at a reservoir temperature T_o = 4500K and area ratio A/A^* = 32. —— Theory; ● experimental value of Y from Hurle et al. (1964) reinterpretated according to MacDonald (1972).

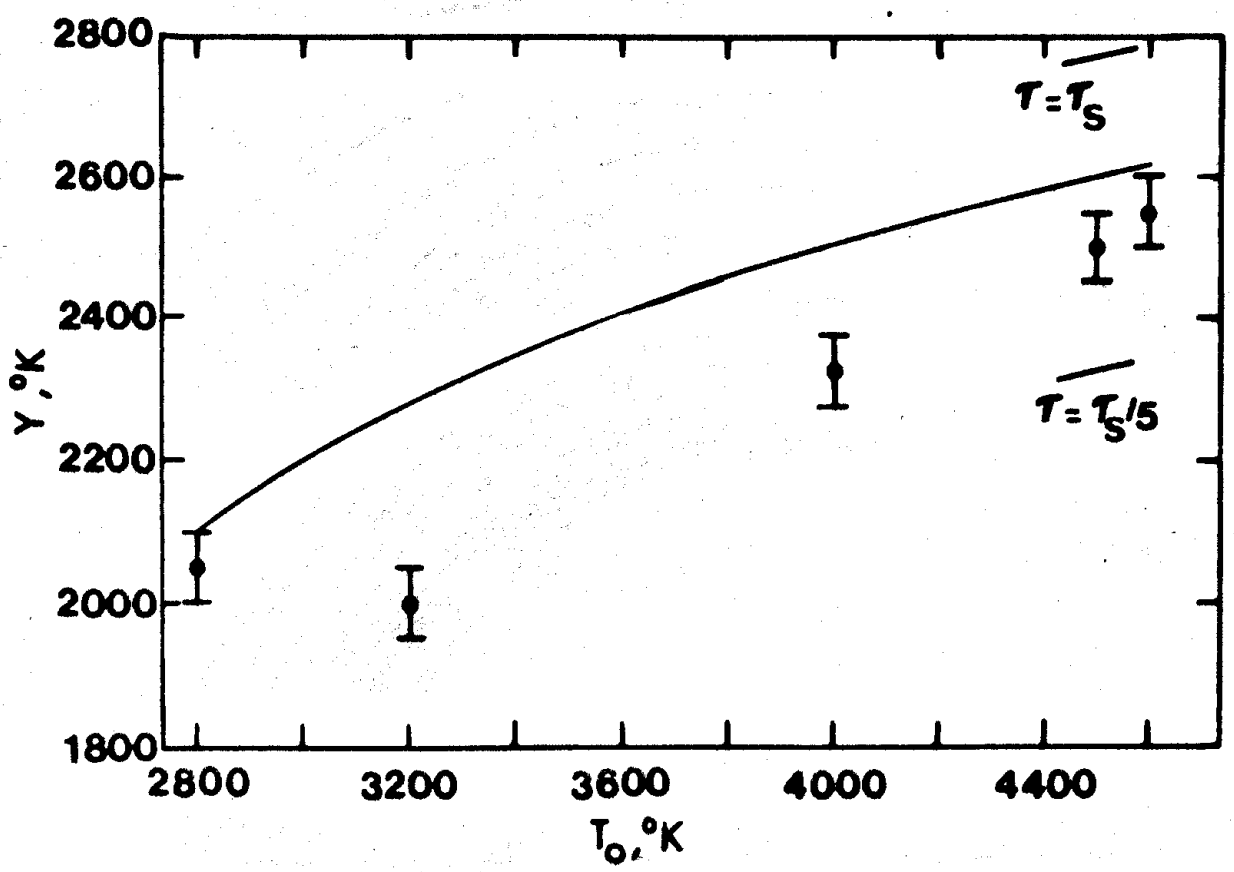

Figure 2.4: Vibrational temperature (Y) vs reservoir temperature (T_o) at P_o = 50 atm and area ratio A/A^* = 8. ——— Theory; ● experimental value of Y from Hurle et al. (1964) reinterpretated according to MacDonald (1972).

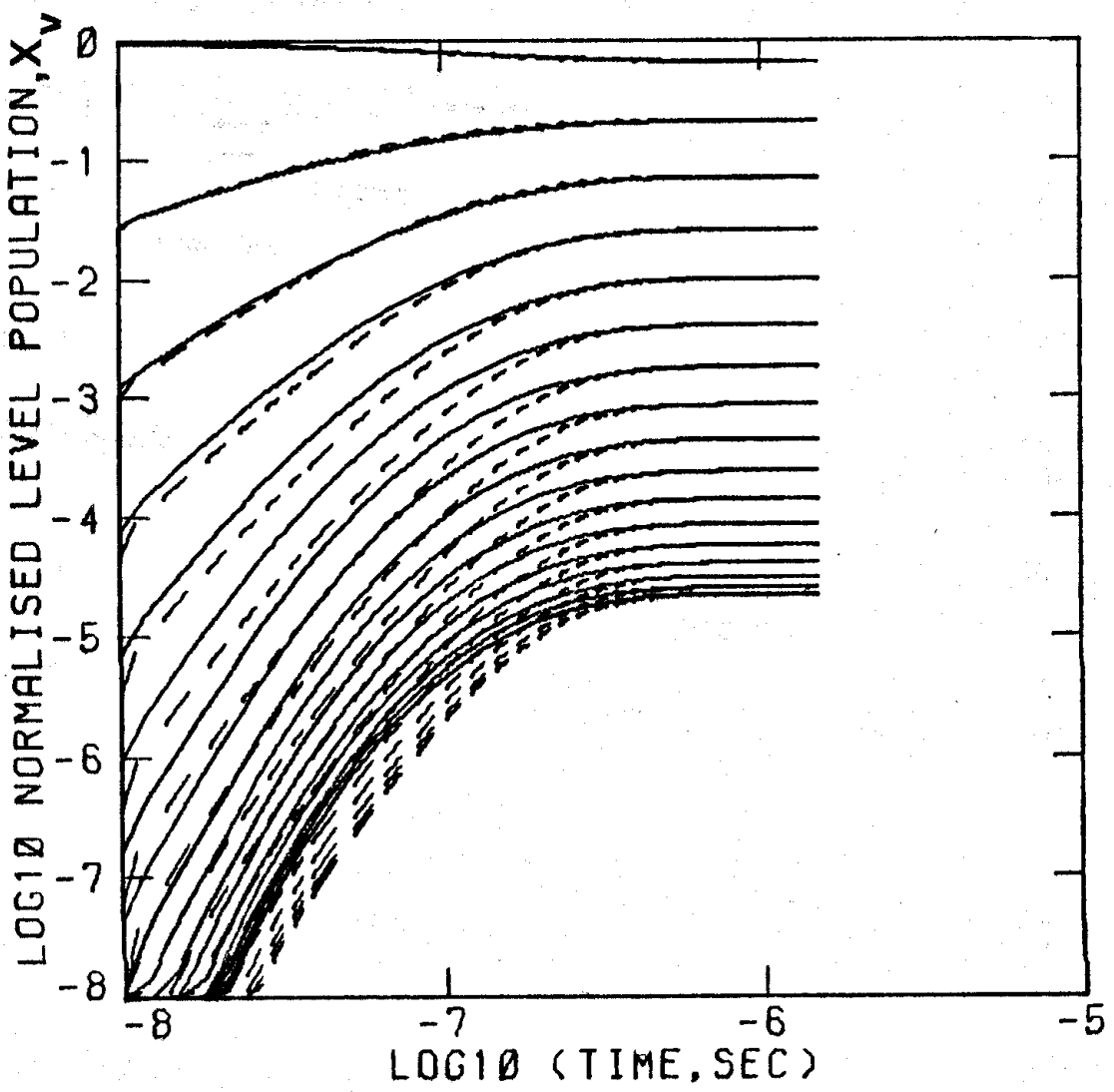

Figure 2.5: Time evolution of vibrational level populations of H_2 at 5000K and 1 atm with no dissociation.——V-T transitions only, --- V-T and V-V transitions. The populations were in a Boltzmann distribution at 300K.

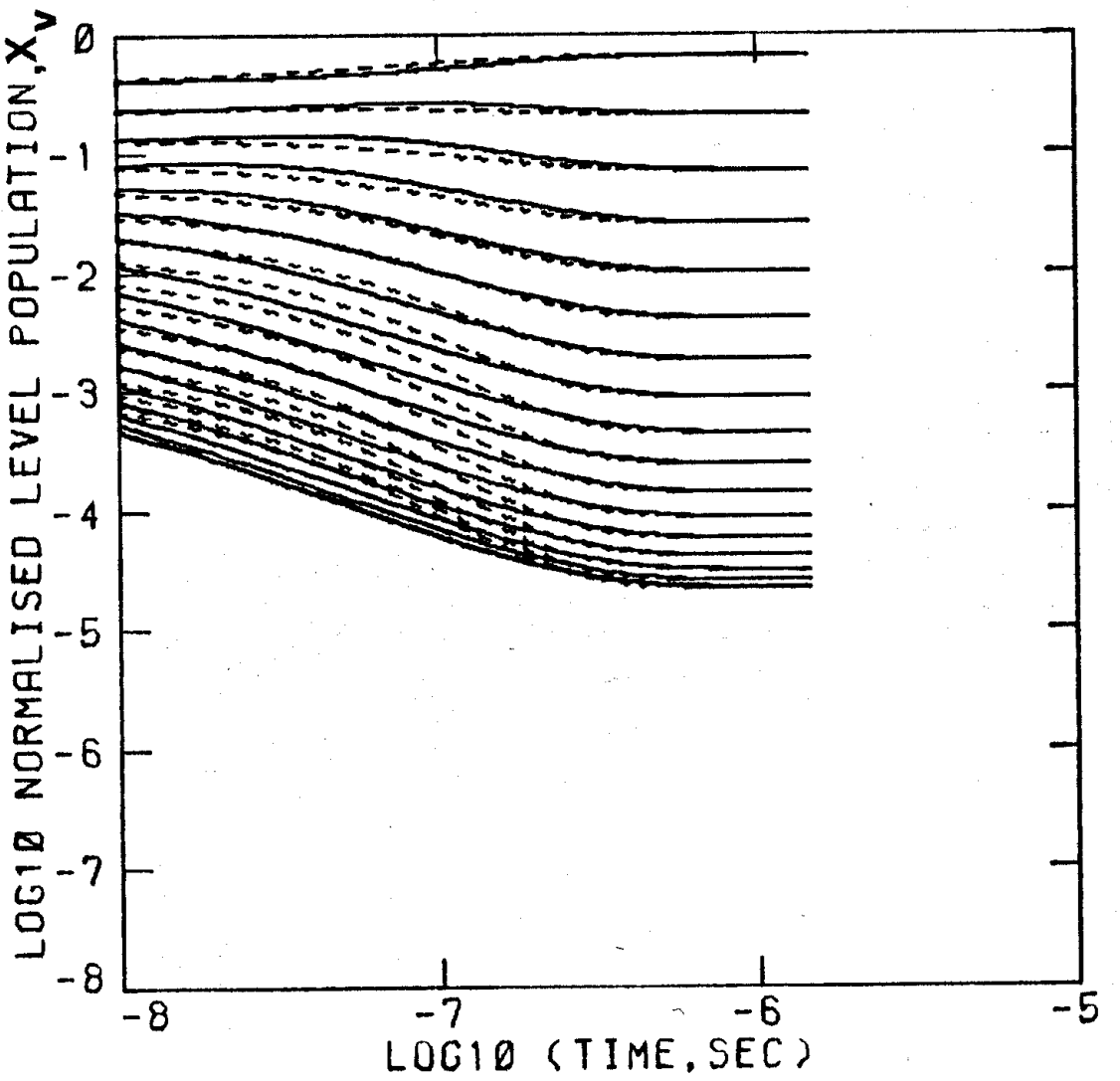

Figure 2.6: Time evolution of vibrational level populations of H_2 at 5000K and 1 atm with no recombination.——V-T transitions only, --- V-T and V-V transitions. The populations were in a Boltzmann distribution at 10000K.

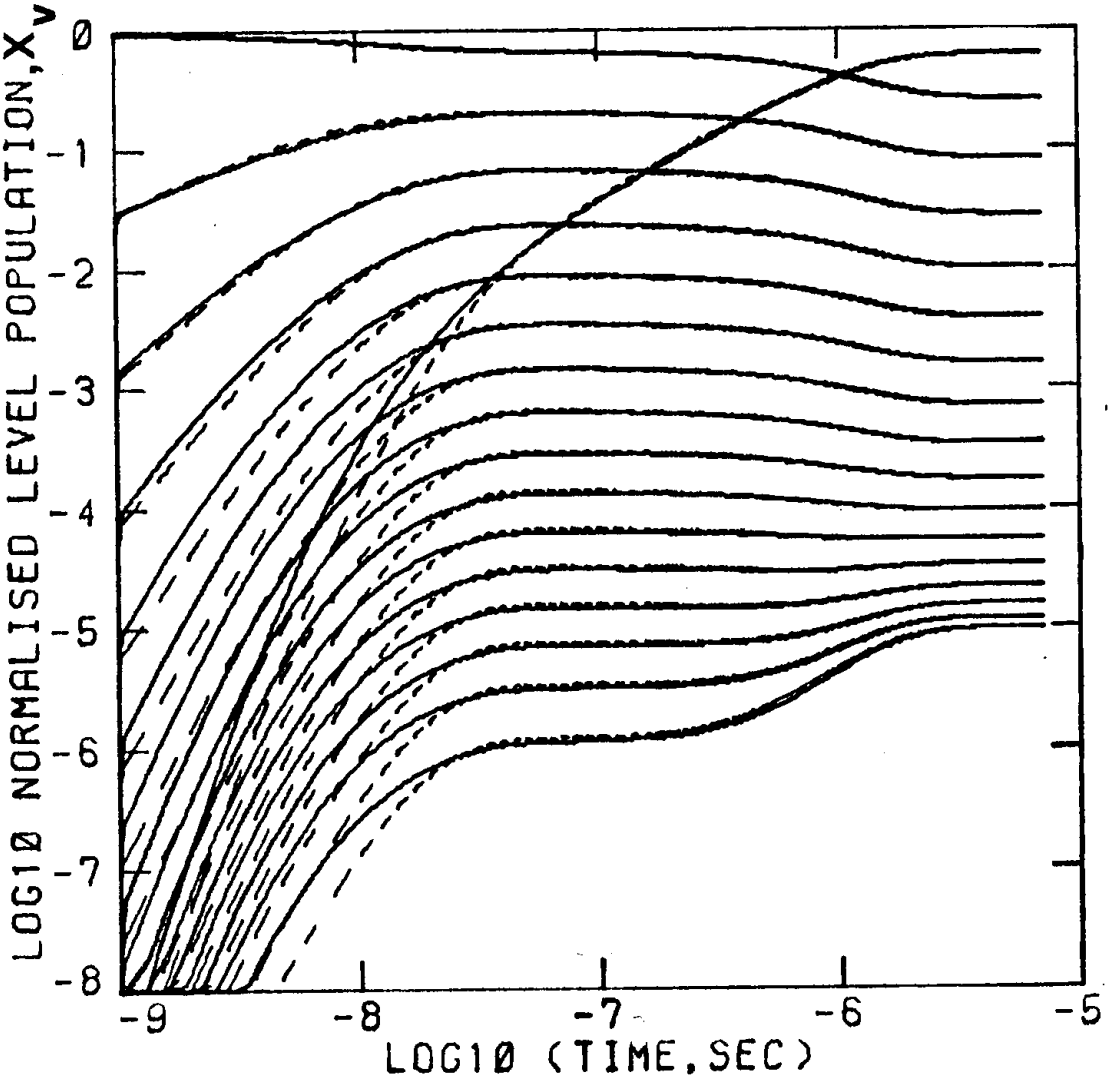

Figure 2.7: Time evolution of vibrational level populations of H_2 at 5000K and 10 atm with dissociation. Half the atom population is also plotted. ——V-T transitions only, --- V-T and V-V transitions. The populations were in a Boltzmann distribution at 300K.

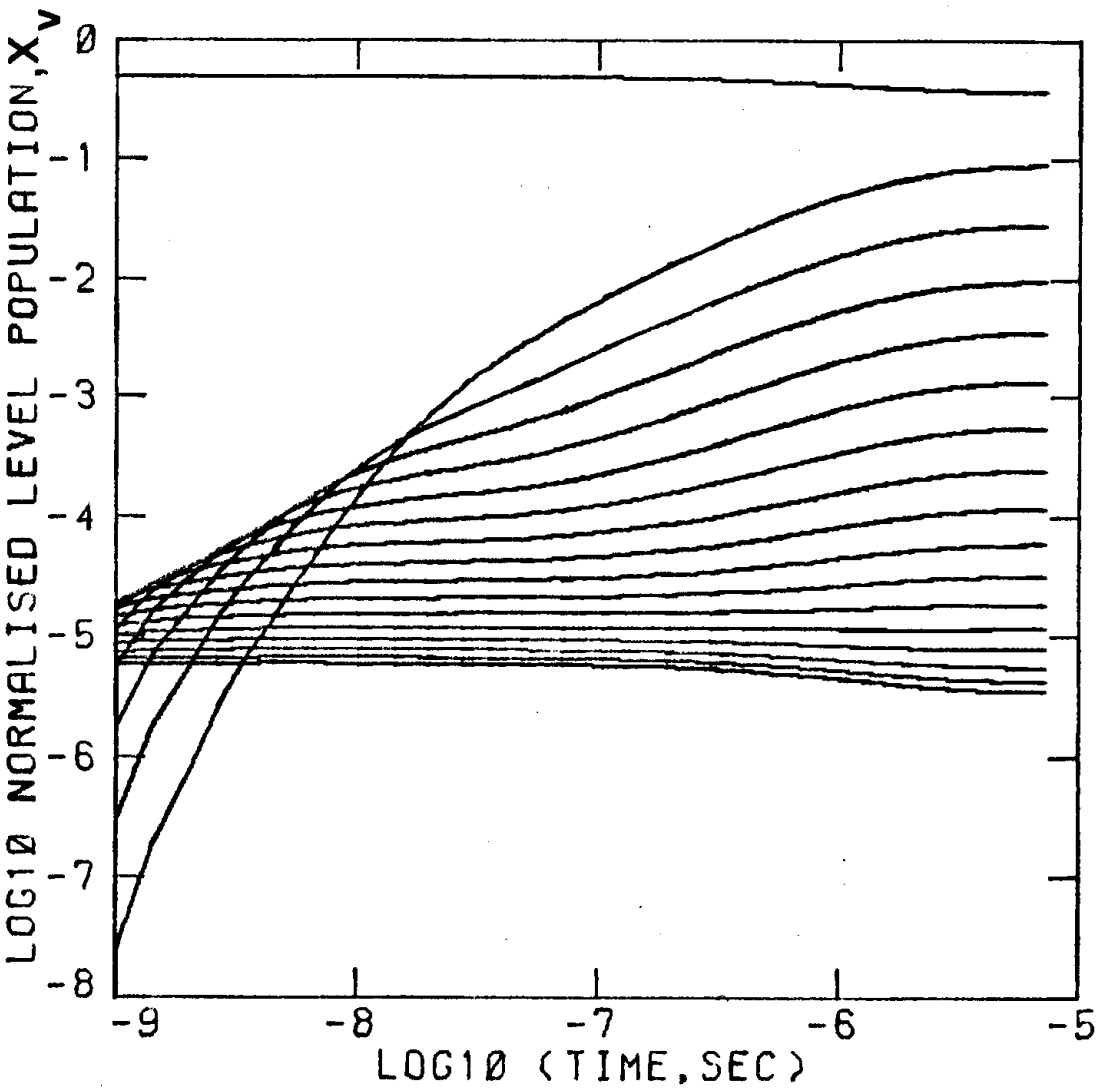

Figure 2.8: Time evolution of vibrational level populations of H_2 at 5000K and 10 atm with recombination. Half the atom population is also plotted.——V-T transitions only,--- V-T and V-V transitions. The populations were in Boltzmann distribution at 10000K. The mole fraction of H_2 was 10^{-8}.

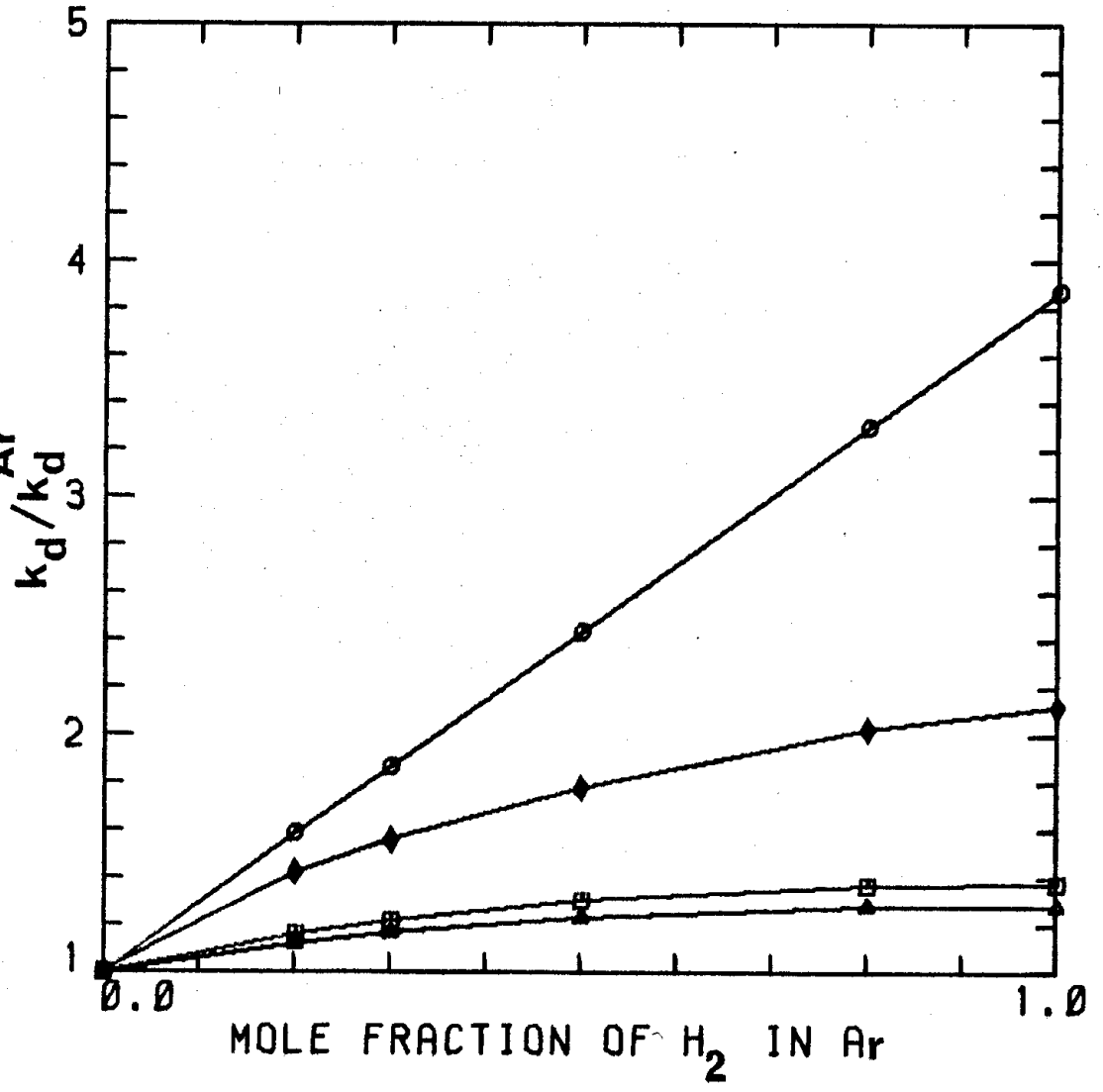

Figure 2.9: Variation of initial dissociation rate of H_2 with mole fraction of H_2 in Ar at 5000K and 1 atm. —▲— V-T transitions only, —□— V-T and V-V transitions, —◆— V-T and V-V transitions with q equal to 100, —○— V-T transitions only, with equal normalised V-T transition probabilities for H_2-H_2 and H_2-Ar collisions.

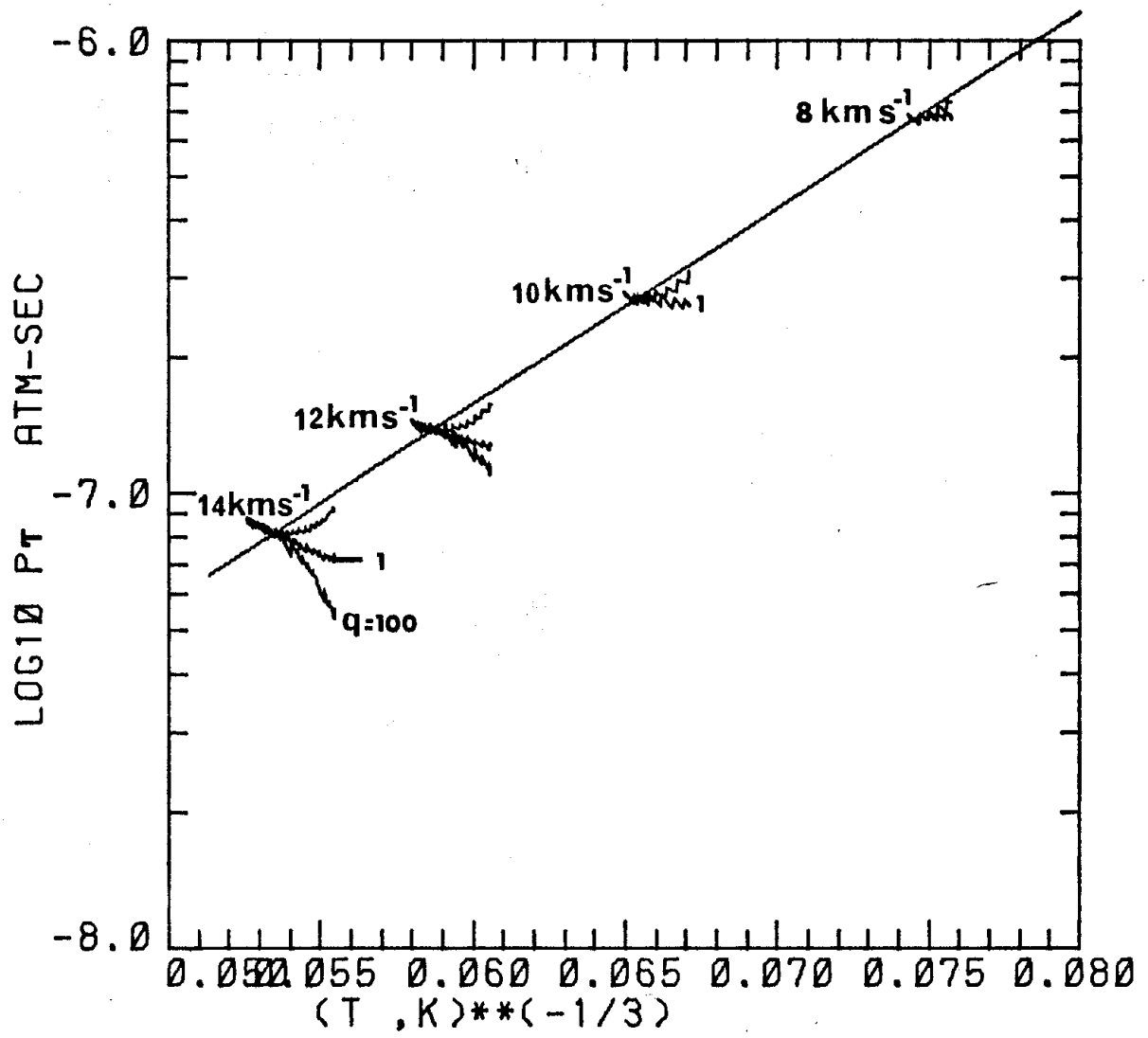

Figure 2.10: Vibrational excitation rates of H_2. The straight line is the experimental value of Kiefer and Lutz (1966b). Results of four shocks in 5 torr initial pressure of H_2 at 300K are plotted. The slowest rate for each shock is for V-T transitions only. The effect of V-V transitions is shown by varying q.

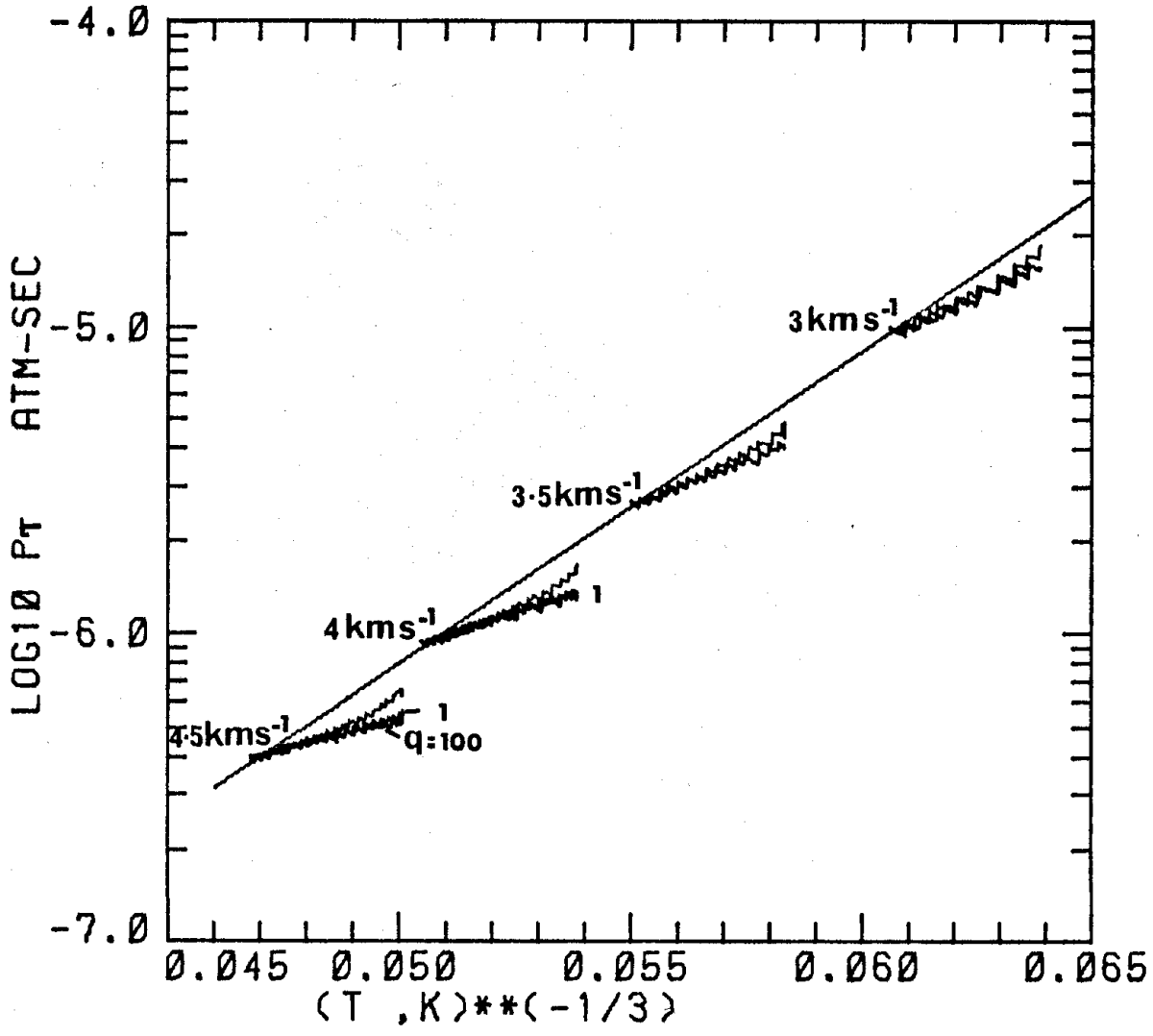

Figure 2.11: Vibrational excitation rates of N_2. The straight line is the experimental value of Appleton (1967). Results of four shocks in 5 torr initial pressure of N_2 at 300K are plotted. The slowest rate for each shock is for V-T transitions only. The effect of V-V transitions is shown by varying q.

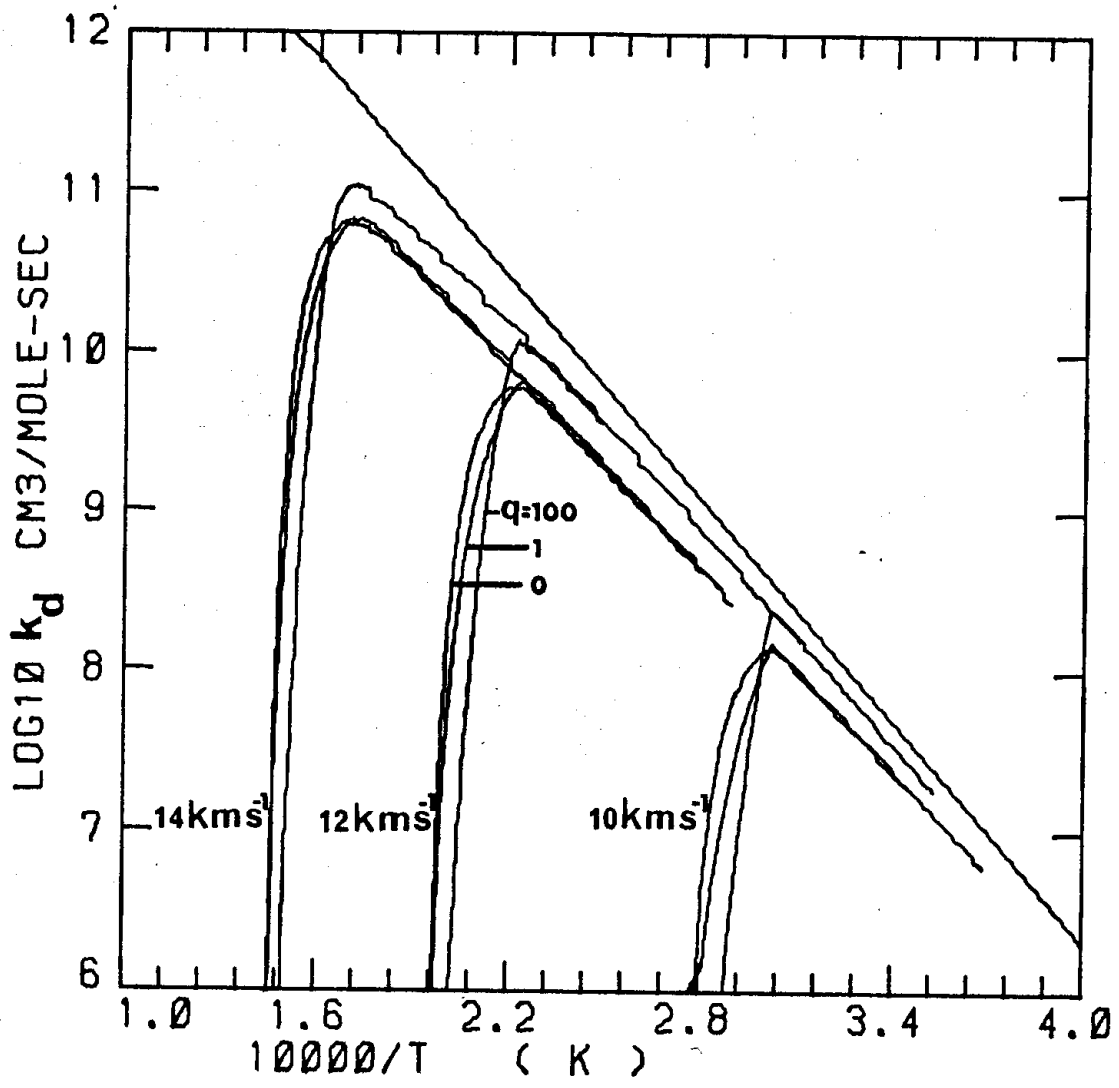

Figure 2.12: Dissociation rate coefficient k_d of H_2. For comparison the experimental value of k_d H_2 given by Breshears and Bird (1973a) is shown. Results of three shocks in 5 torr initial pressure of H_2 at 300K are plotted. The effect of V-V transitions is shown by varying q.

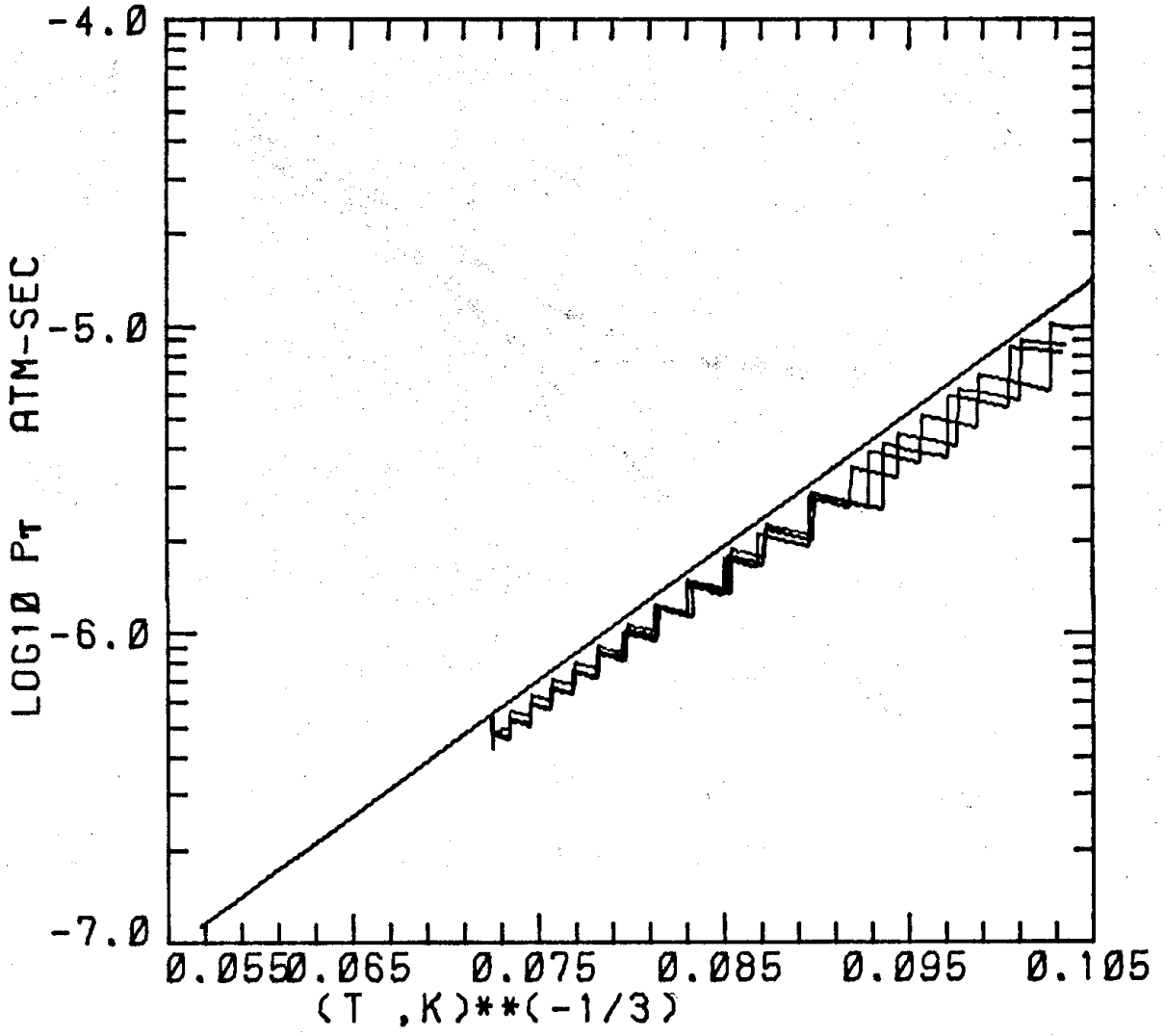

Figure 2.13: Vibrational de-excitation rates of H_2. The straight line is the experimental value of Kiefer and Lutz (1966b). The reservoir conditions are 3000K and 50 atm. The rates for V-T transitions only, V-T and V-V transitions and V-T and V-V transitions with q equal to 10 are seen to be nearly identical.

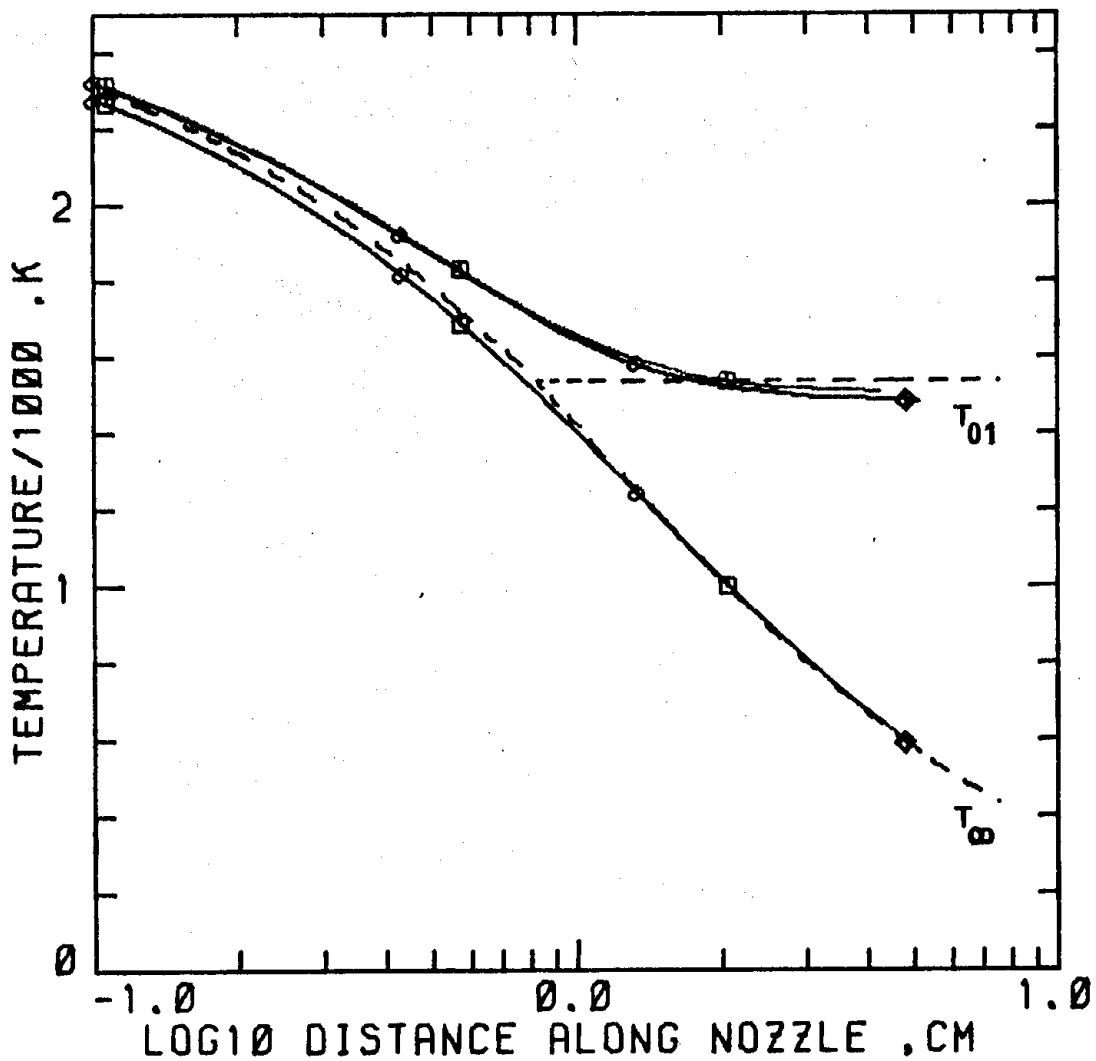

Figure 2.14: Vibrational and translational temperature along the nozzle. The reservoir conditions are 3000K and 50 atm.---calculations using Lordi et al. (1966), —⊟— V-T transitions only, —◇— V-T and V-V transitions.

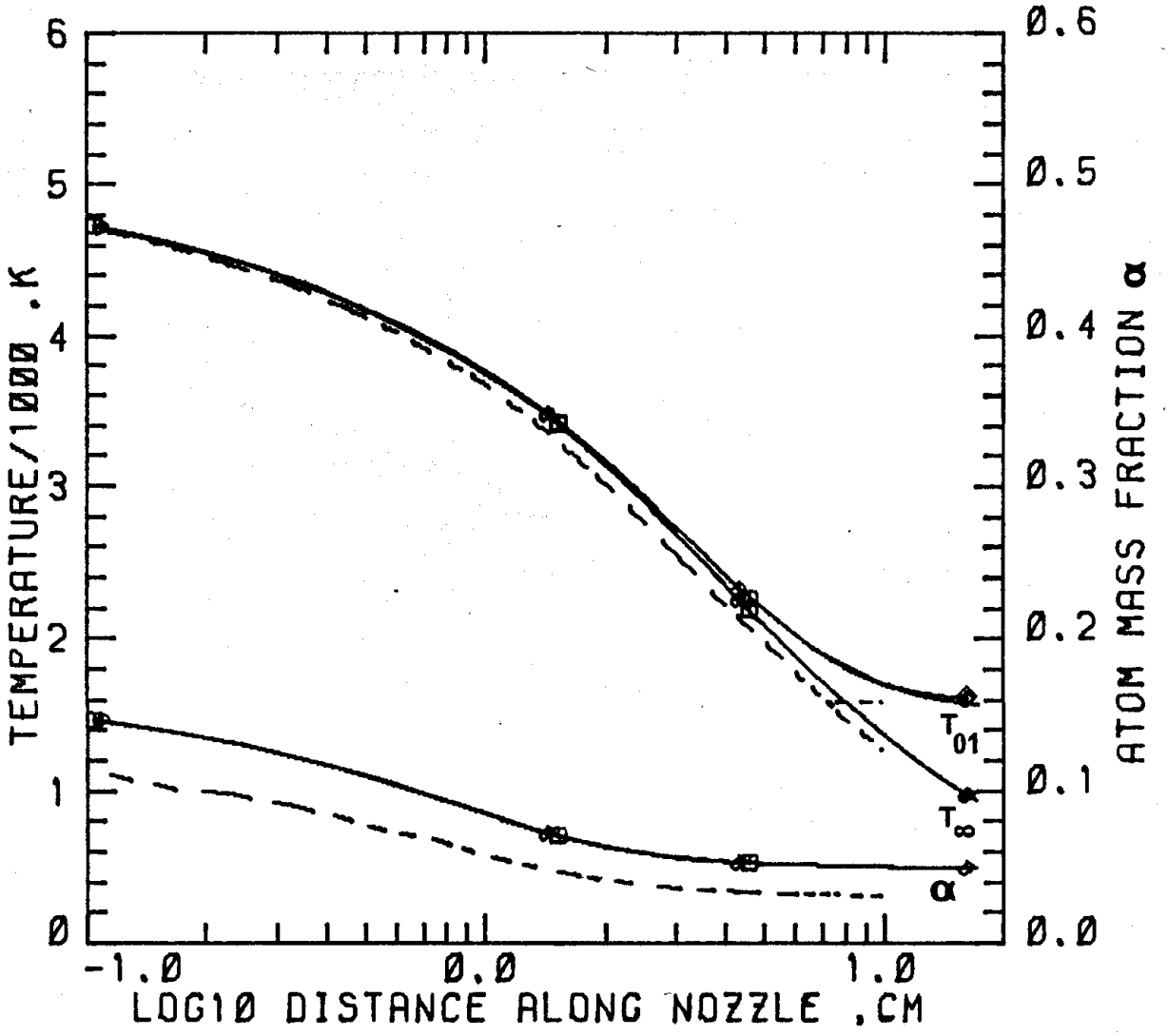

Figure 2.15a: Atom mass fraction, vibrational and translational temperature along the nozzle --- calculations using Lordi et al. (1966), —⊟— V-T transitions only, —◇— V-T and V-V transitions.
The reservoir conditions are 5000K and 200 atm.

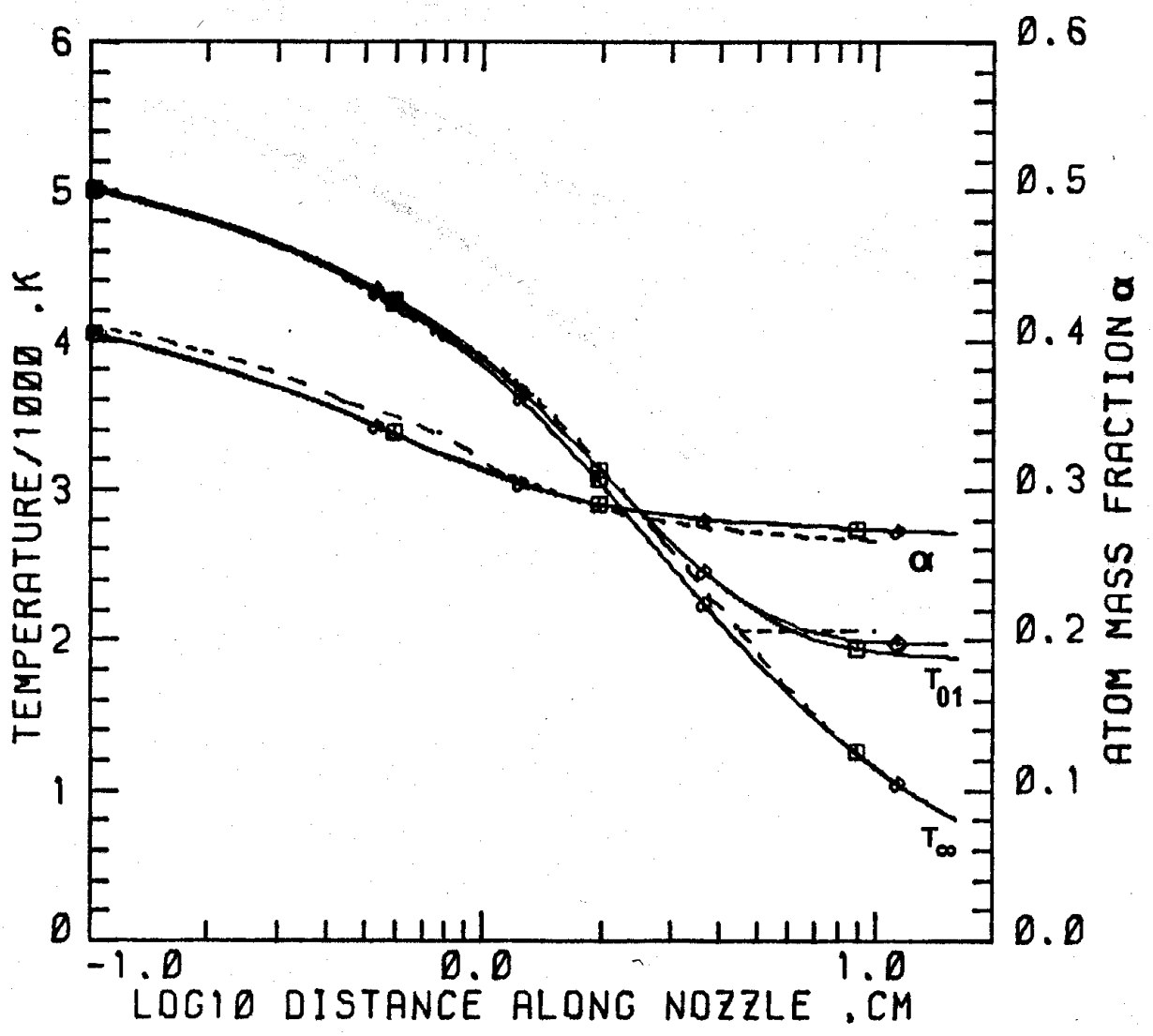

Figure 2.15b: Atom mass fraction, vibrational and translational temperature along the nozzle. The reservoir conditions are 6000K and 200 atm.

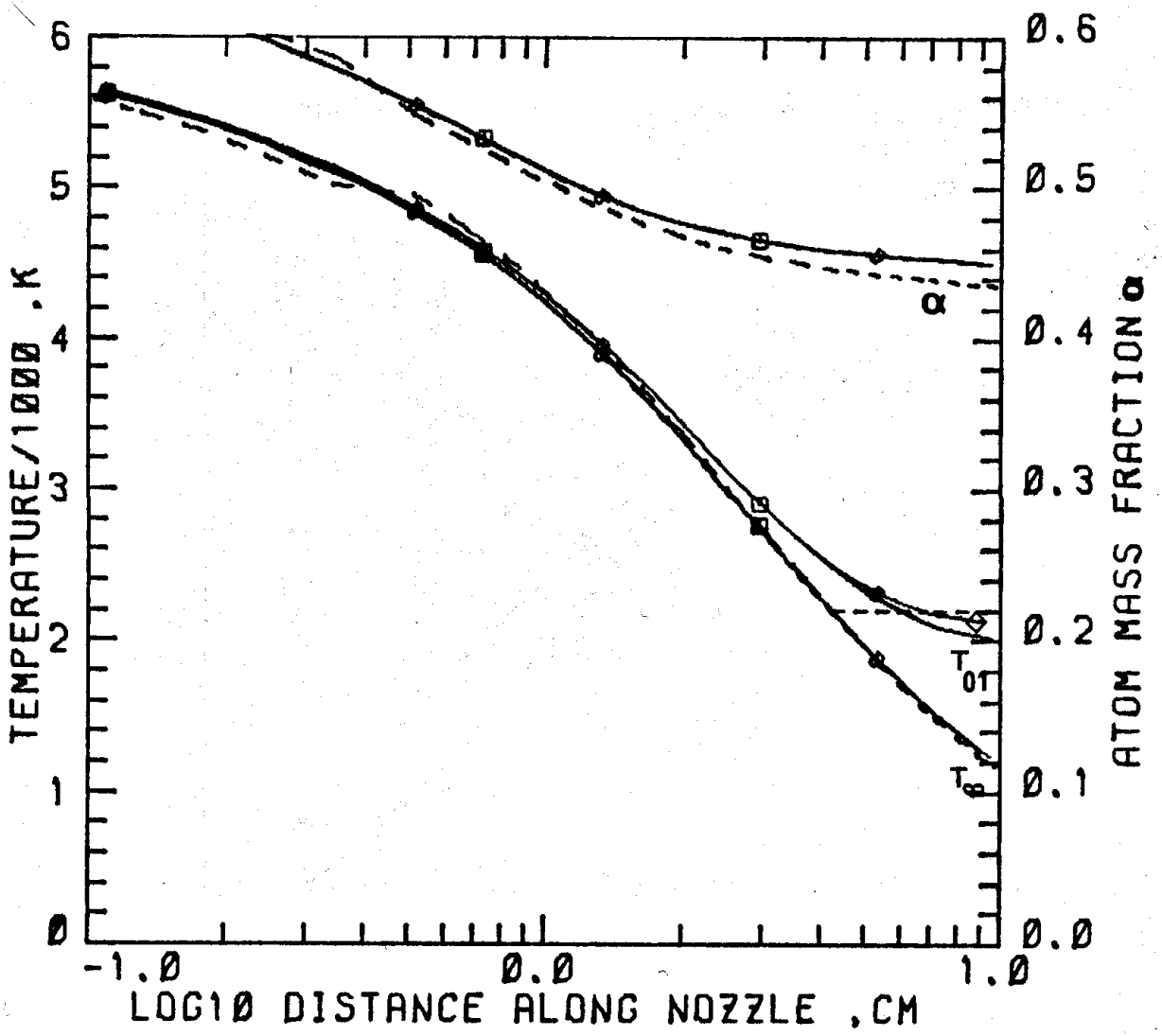

Figure 2.15c: Atom mass fraction, vibrational and translational temperature along the nozzle. The reservoir conditions are 7000K and 200 atm.

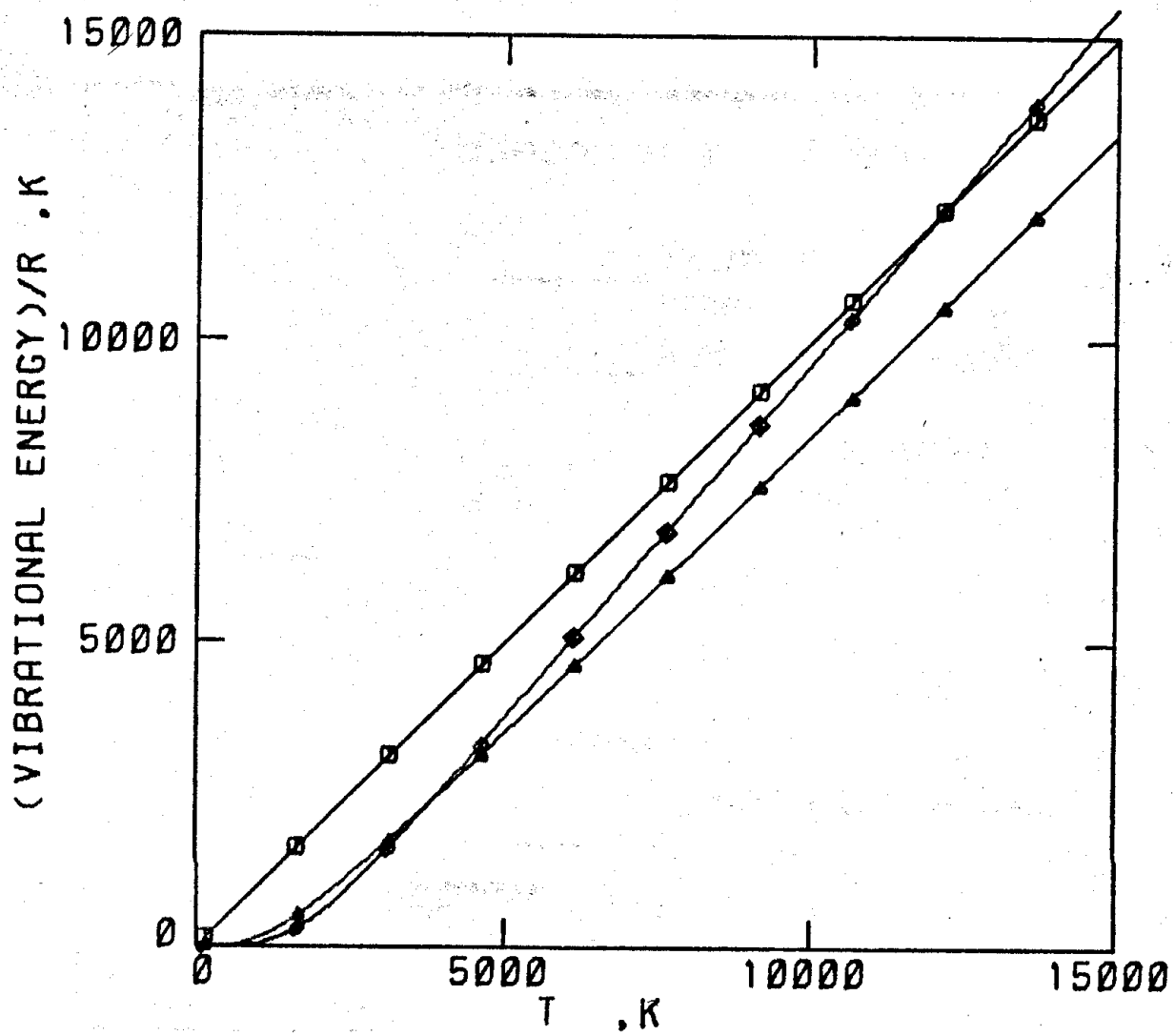

Figure 2.16: Comparison between the vibrational equilibrium energy, per mole, of the SHO and the MO representation of N_2 for temperatures up to 15000K. —◇— MO, —▲— SHO, and —□— RT.

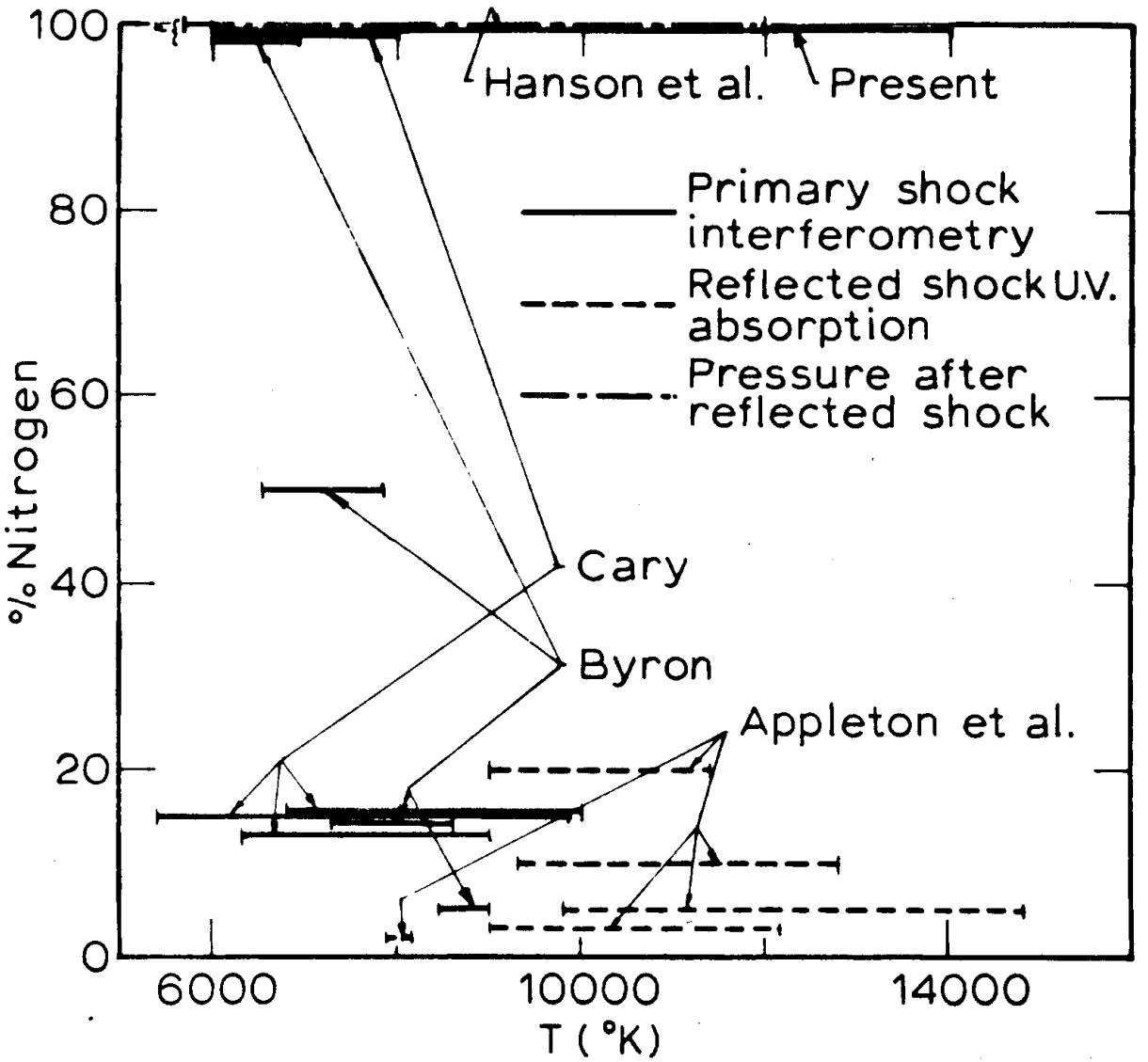

Figure 3.1: Range of temperature and inert gas dilution of different dissociation rate measurements.

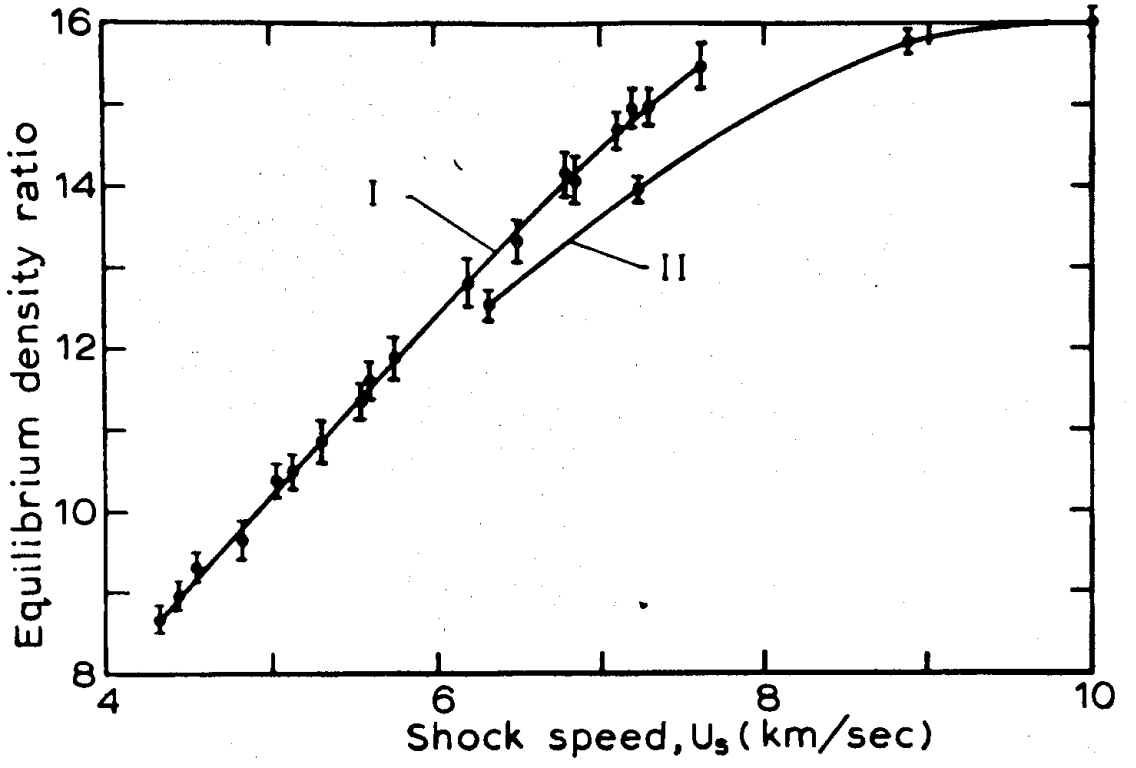

Figure 3.2: Ratio of equilibrium to initial density as a function of shock speed for two driver conditions. Curve I, 2700 lb/in^2, curve II, 10500 lb/in^2 diaphragm burst pressure. ——— Calculated, ● measured.

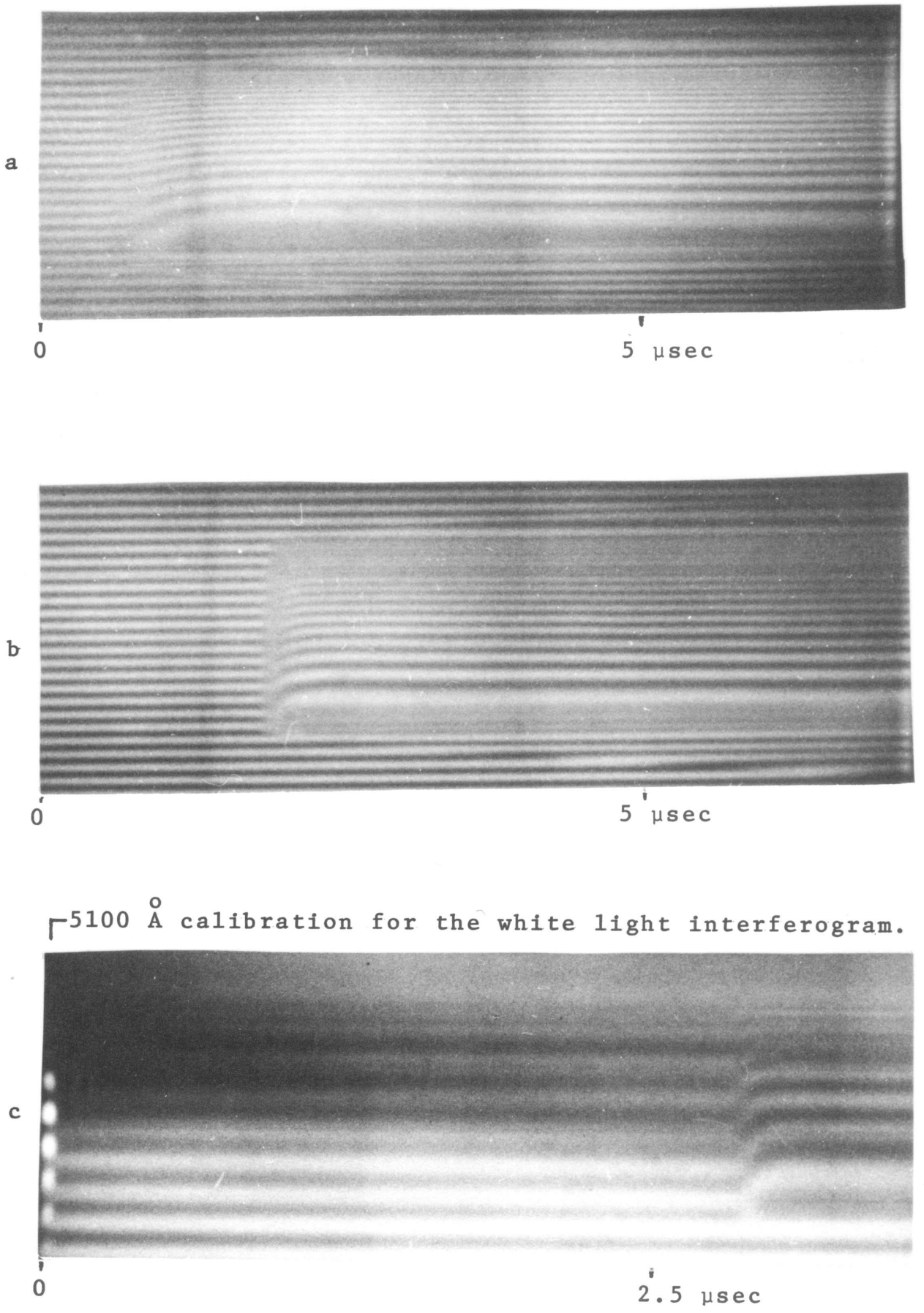

Figure 3.3: Three time-resolved interferograms of nitrogen dissociation behind a shock.

a 4.80 km sec^{-1}, 31 torr, 298.2K.
b 5.60 km sec^{-1}, 19 torr, 298.2K.
c 7.31 km sec^{-1}, 5 torr, 300.2K.

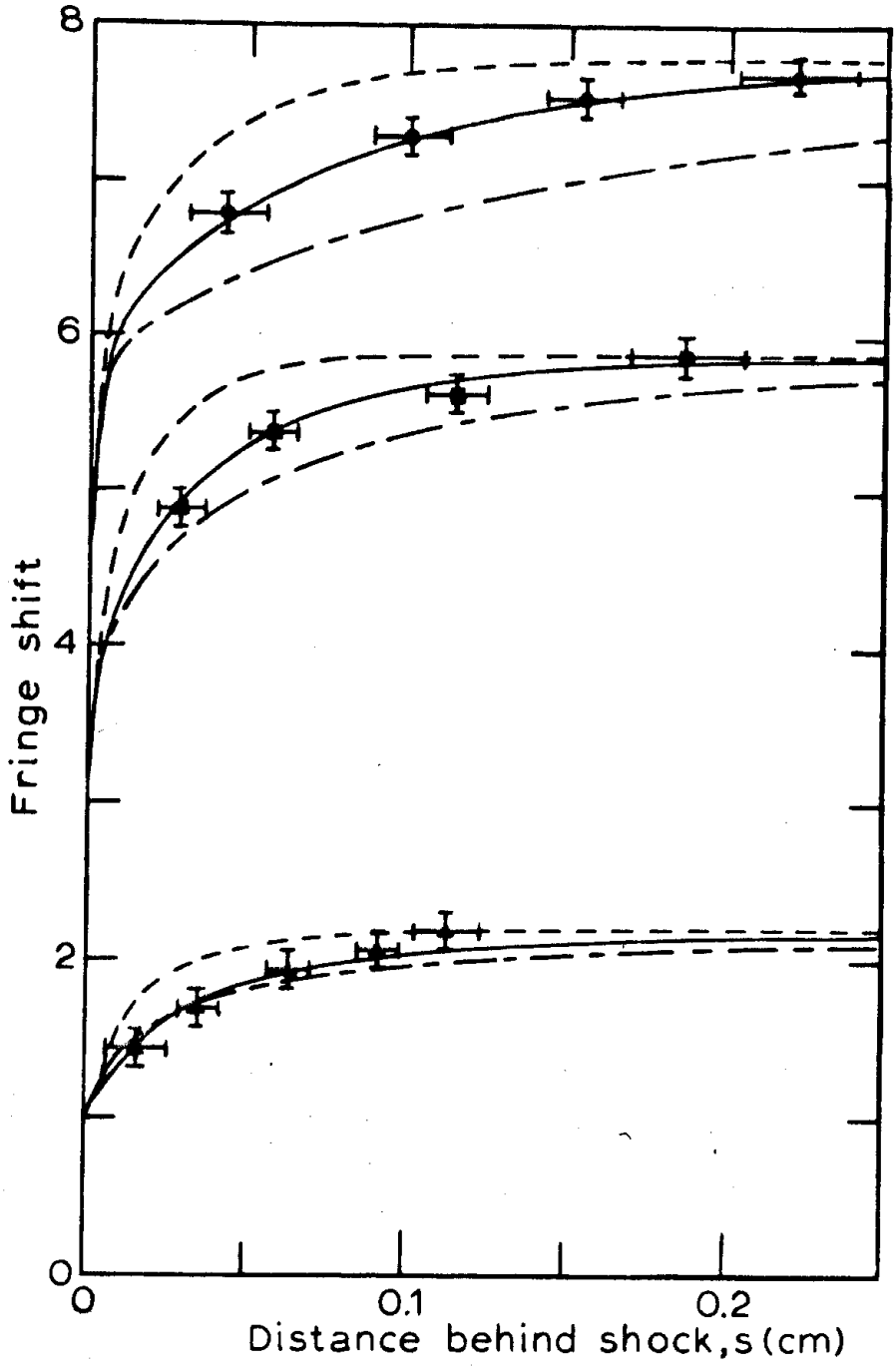

Figure 3.4: Calculated and measured fringe shift in the relaxation zone for three shock speeds: ● 4.80 km sec^{-1}, 31 torr; ■ 5.60 km sec^{-1}, 19 torr; ▲ 7.31 km sec^{-1}, 5 torr. Calculated curves according to Hanson and Baganoff (1972) ---, Appleton et al. (1968) ____ __ ____, equations 3.2-11 and 12 _____.

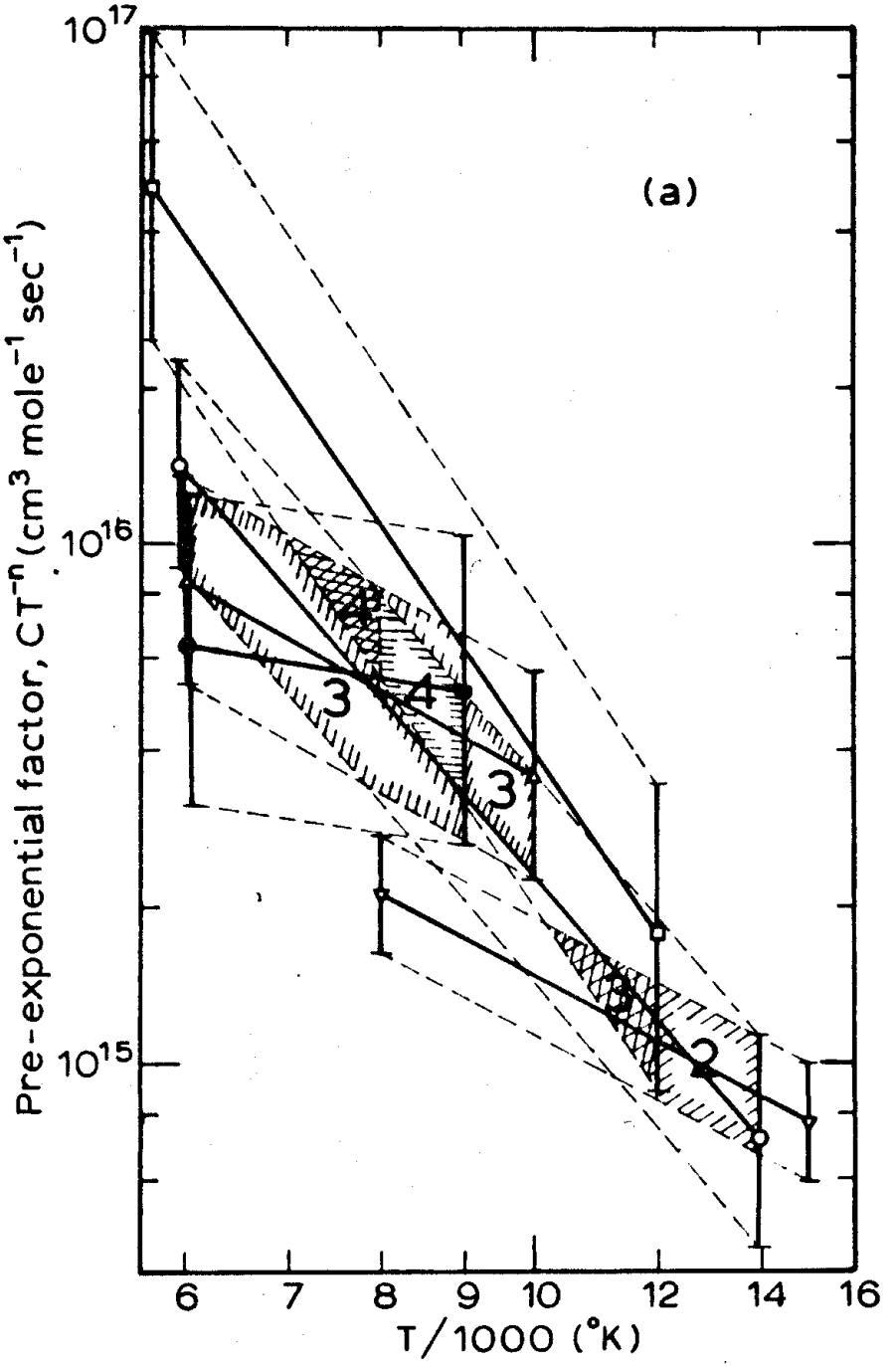

Figure 3.5a: Pre-exponential factor for the rate coefficient $k_d^{N_2}$ versus temperature; □ Hanson and Baganoff (1972), ○ present, △ Cary (1966), ▽ Appleton et al. (1968), ● Byron (1966). The error bars indicate authors' estimated uncertainties. Edge-hatching delineates regions in which 3 or more but not all, authors agree, or that if only 2 authors cover the range, they agree. Cross-hatching indicates where all authors agree. The numbers indicate how many authors agree in the region.

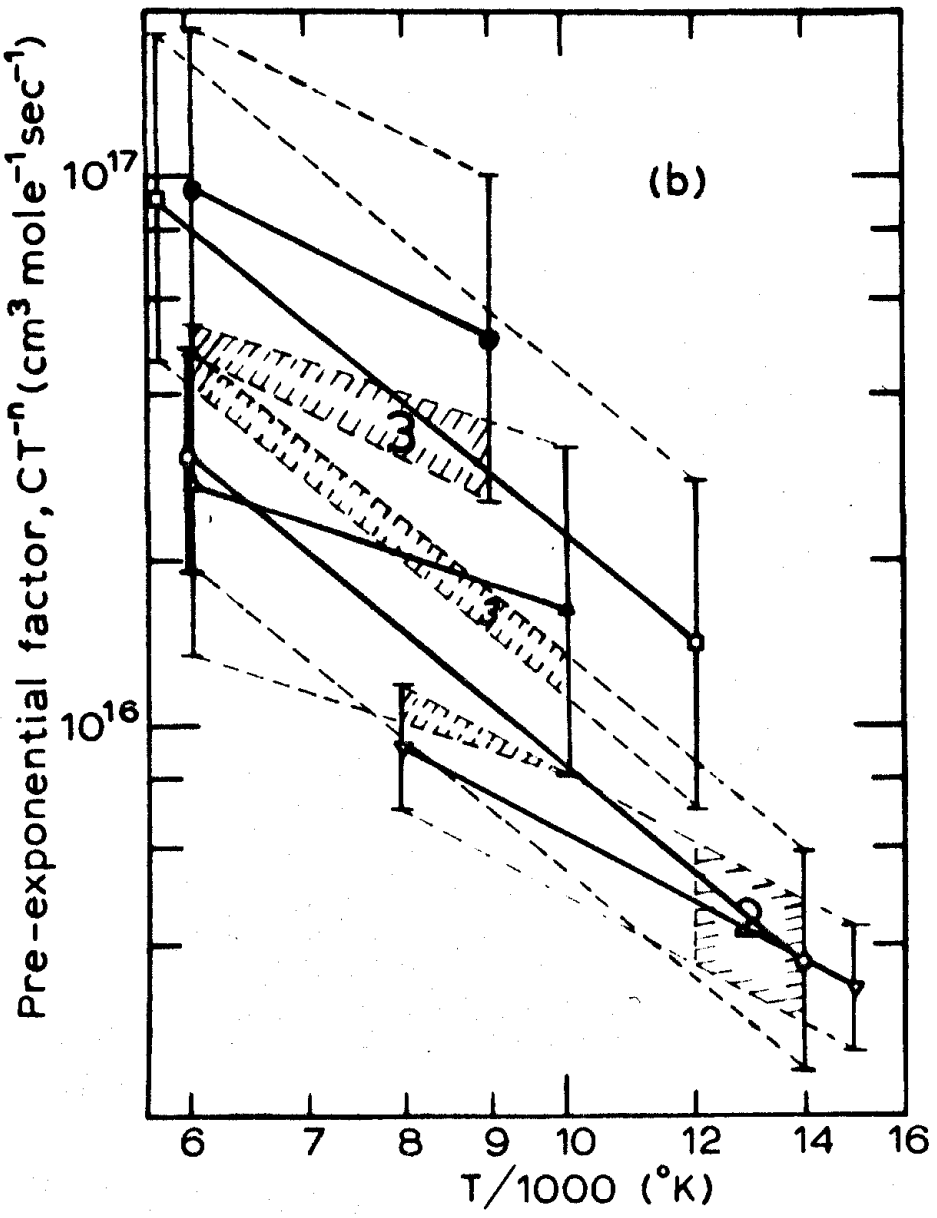

Figure 3.5b: Pre-exponential factor for the rate coefficient k_d^N versus temperature.

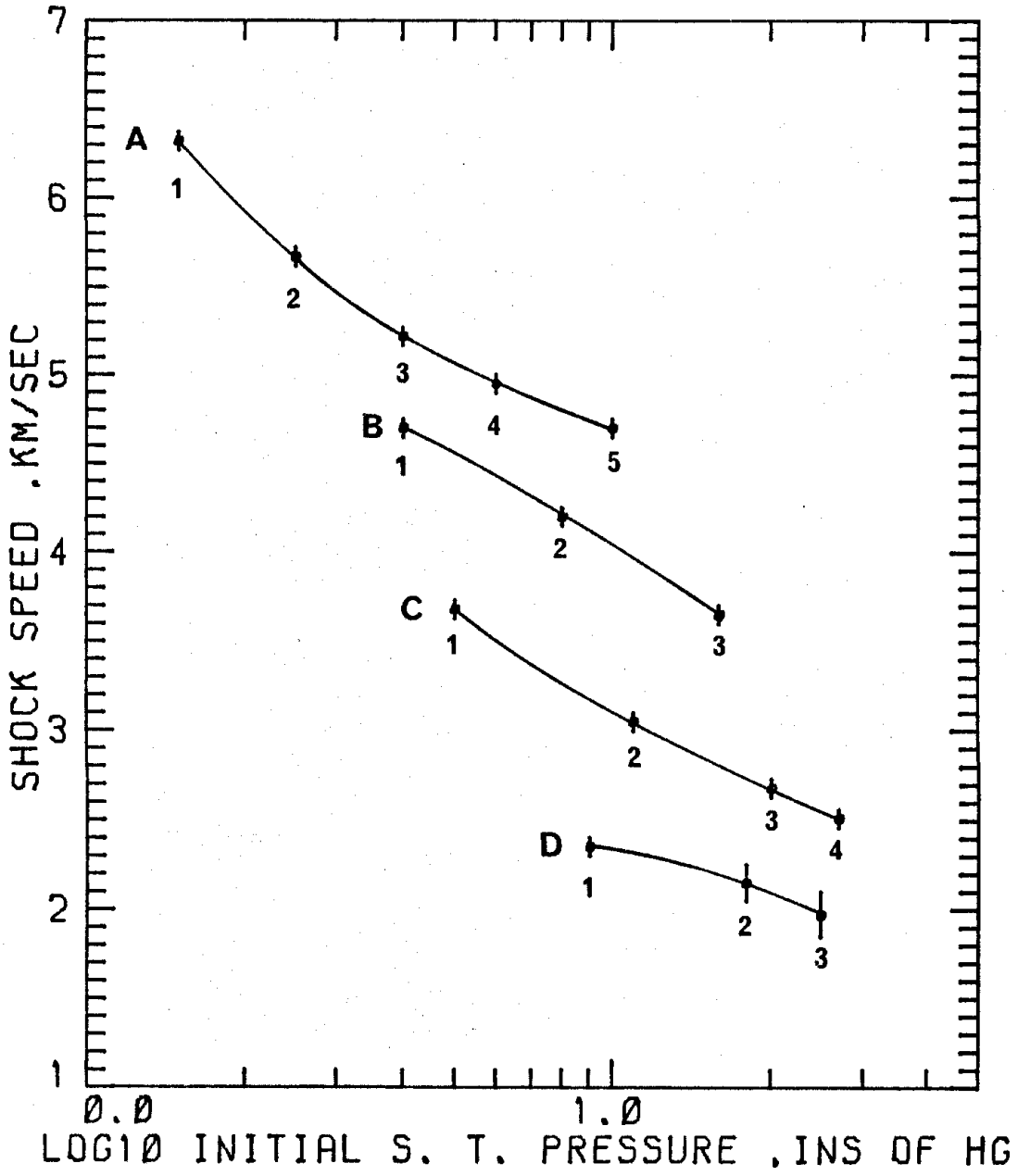

Figure 3.6: Primary shock speed in T2 versus initial shock tube pressure of nitrogen for four operating conditions

A. He driver, p_b = 6800 psi, λ_p = 37

B. He driver, p_b = 3600 psi, λ_p = 29

C. He driver, p_b = 1700 psi, λ_p = 14

D. Ar driver, p_b = 6800 psi, λ_p = 37.

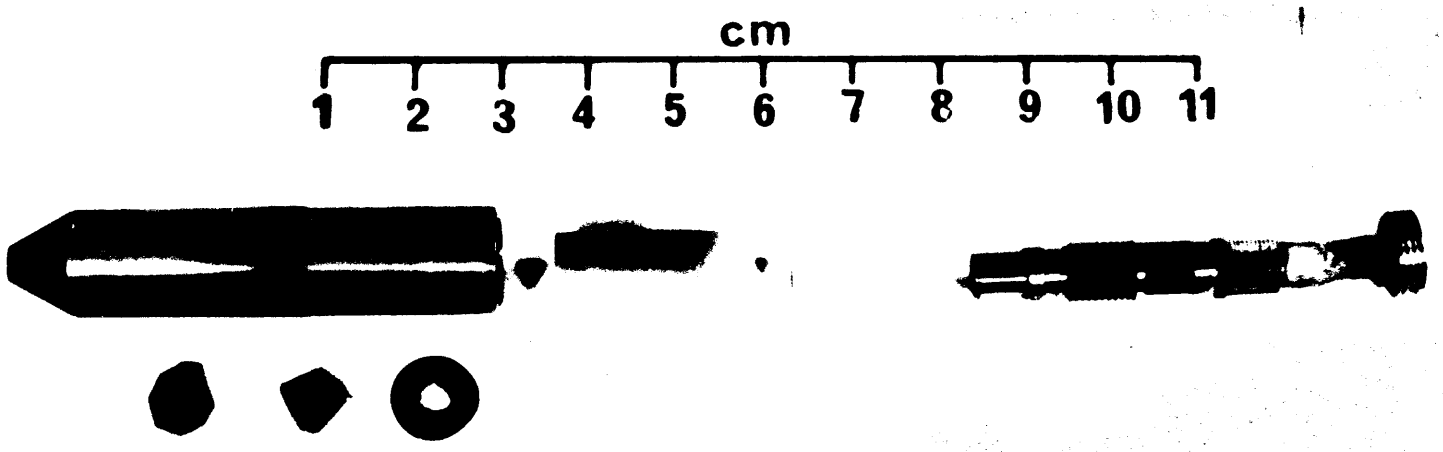

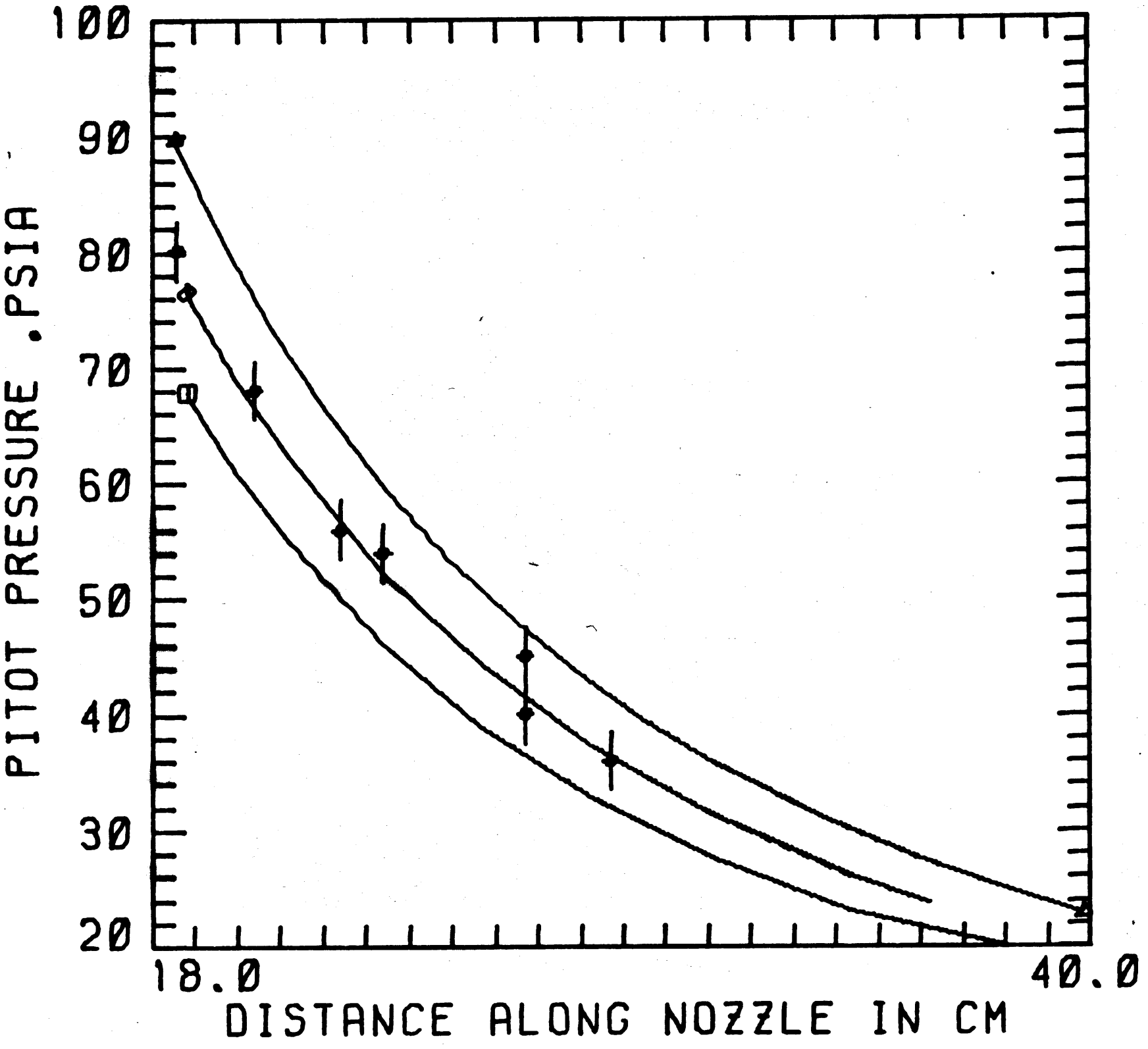

△ 13 deg nozzle

□ 15 deg nozzle

◇ 14 deg nozzle

Figure 3.7: Pitot pressure probe and results of an axial Pitot pressure survey. The nozzle stagnation conditions are T_o = 4400K and P_o = 227 atm.

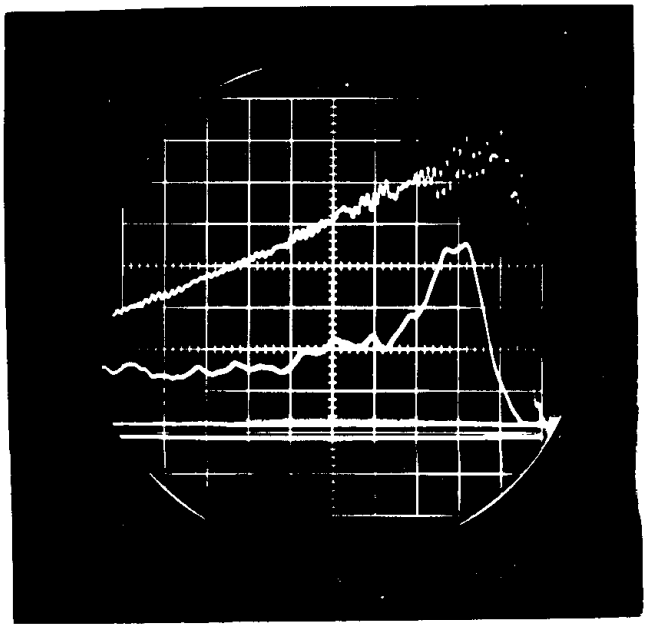

Nozzle stagnation condition = B2

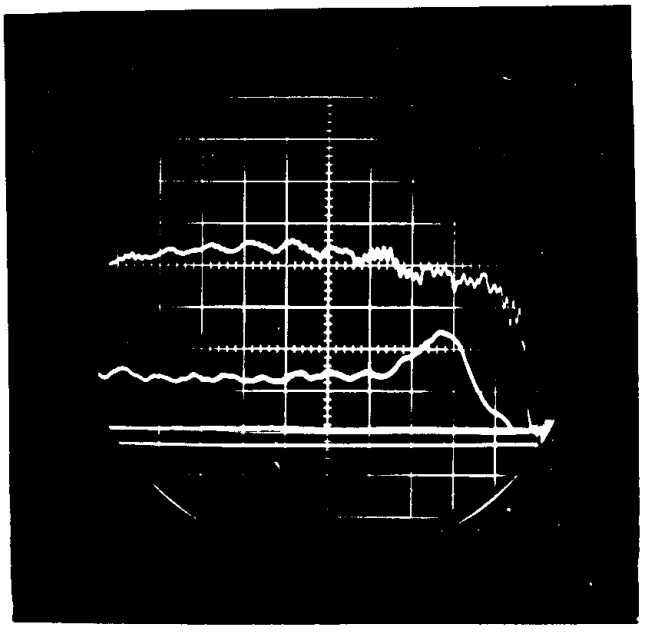

Nozzle stagnation condition = C1

Figure 3.8: Static pressure variation with time, measured from shock reflection in the shock tube.

Vertical scale: Stagnation pressure - 35 atm/div
Static pressure - 0.143 psi/div

Horizontal scale: Time, increasing from right to left - 100 μsec/div

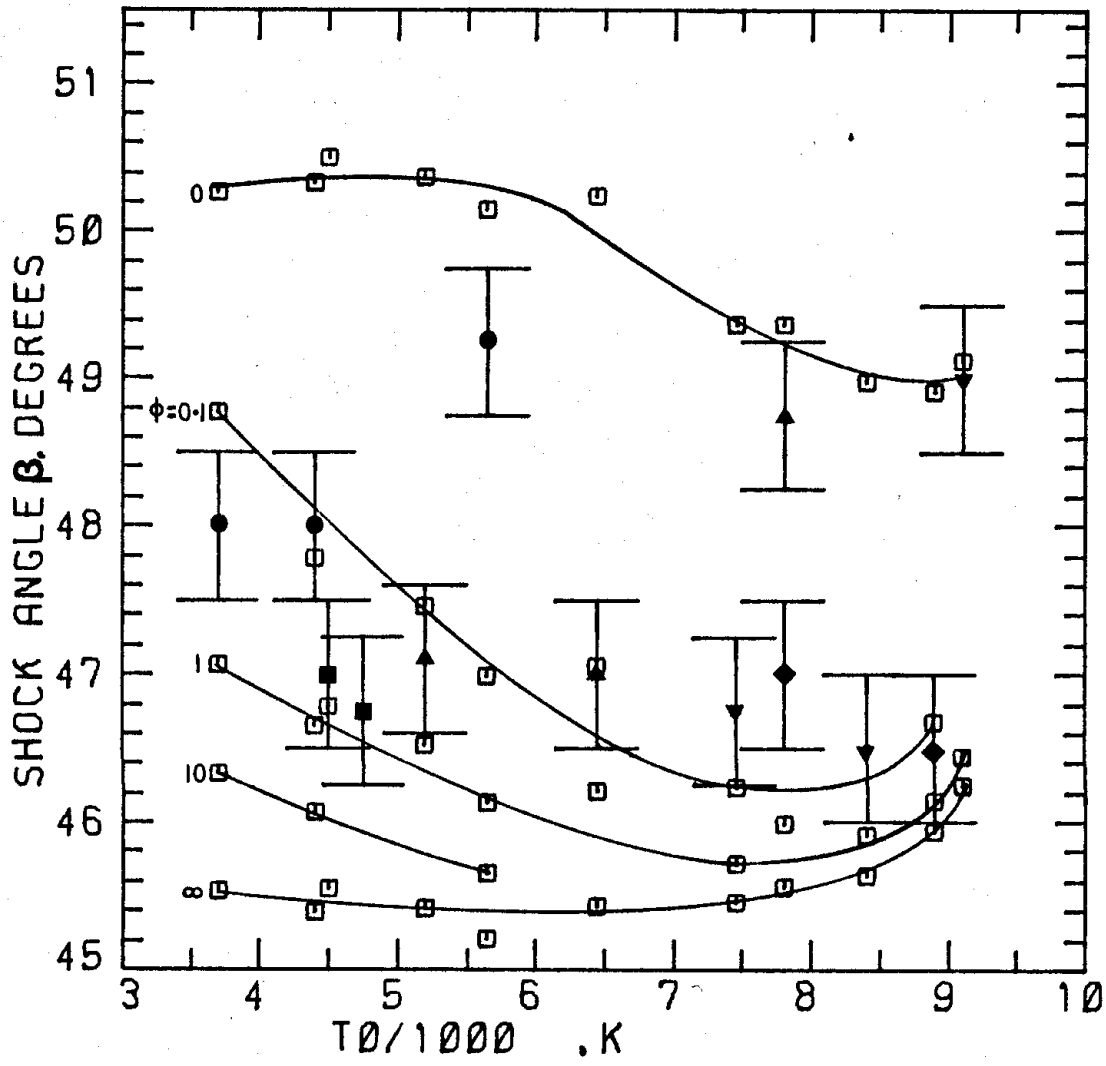

Figure 3.9: Calculated and measured shock angle on a 35° wedge for the range of stagnation temperature T_o. ——— represents a free-hand fit to the calculated points ⊡ . The time, after shock reflection, of each measured interferogram is indicated: ● 500 μsec, ▲ 350 μsec, ■ 300 μsec, ◆ 225 μsec ▼ 200 μsec. ϕ represents the ratio of vibrational de-excitation rate to excitation rate used in the calculations. The error bar of 300K for T_o, above 4500K, is considered to be pessimistic.

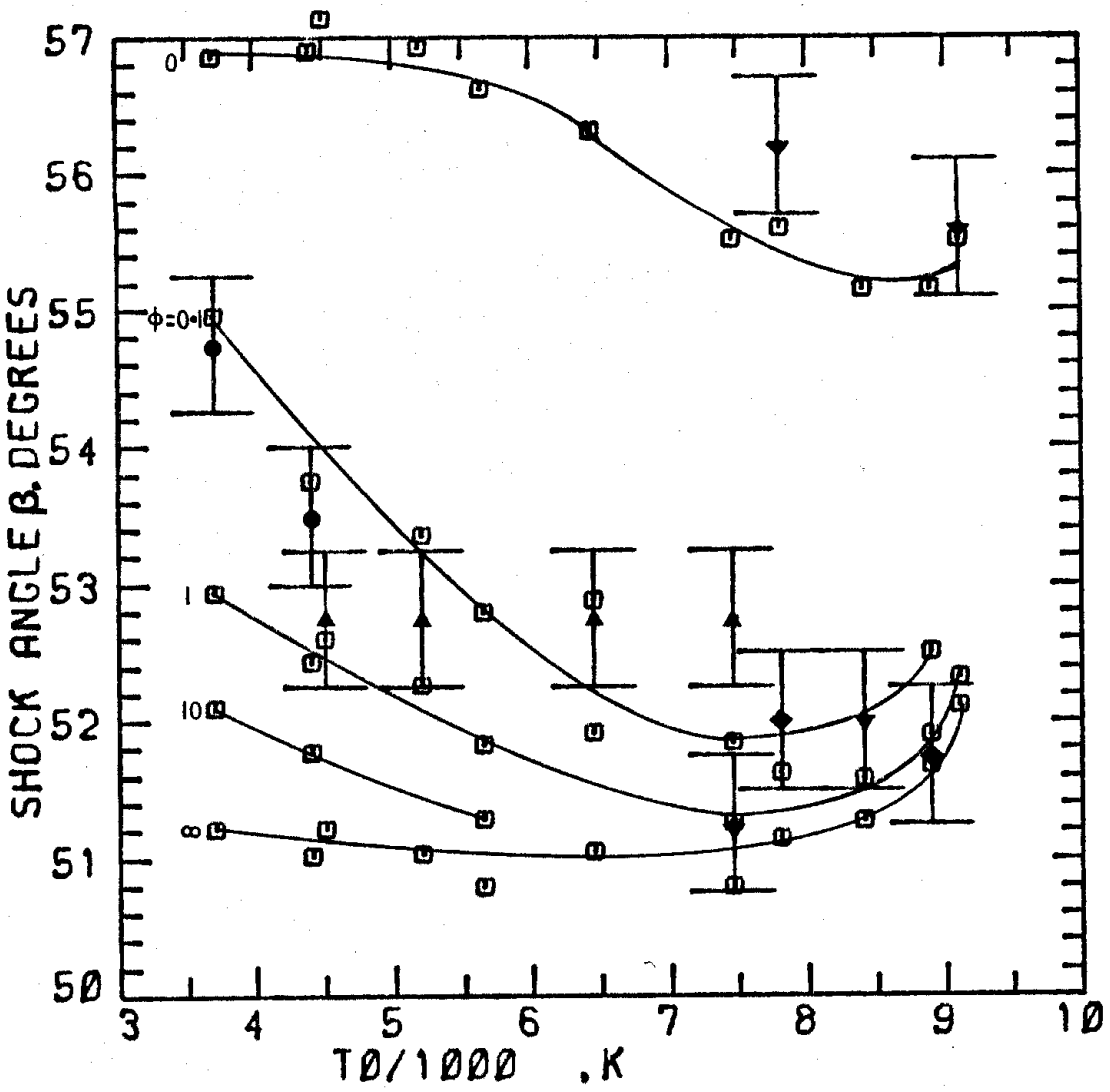

Figure 3.10: Calculated and measured shock angle on a 39° wedge for the range of stagnation temperature T_o. The description is the same as Figure 3.9.

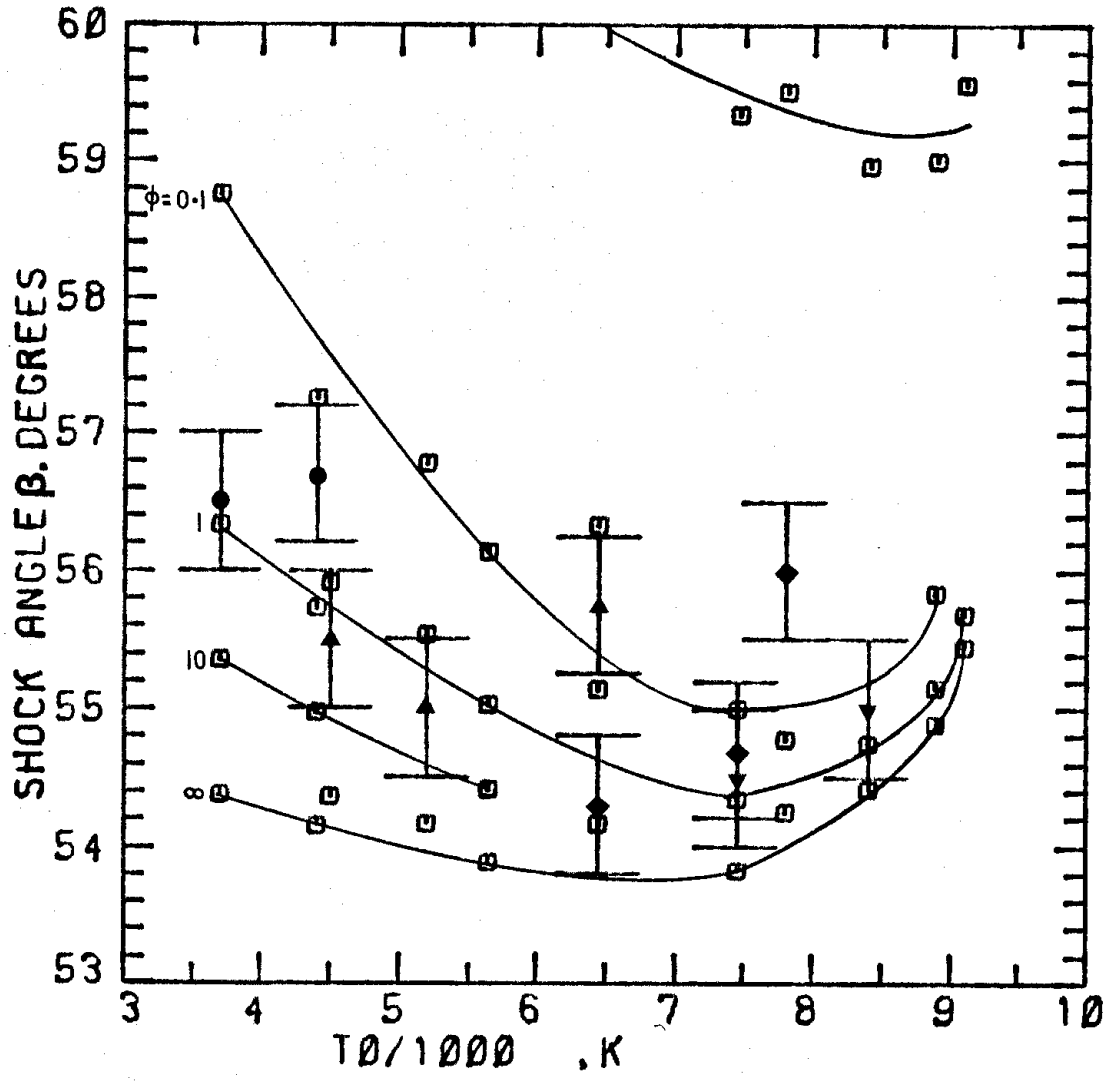

Figure 3.11: Calculated and measured shock angle on a 41° wedge for the range of stagnation temperature T_o. The description is the same as Figure 3.9.